The PMA Phorbol Ester Tumor Promoter Increases Canonical Wnt Signaling Via Macropinocytosis

Nydia Tejeda-Muñoz[1,3*], Yagmur Azbazdar[1,3], Julia Monka[1], Grace Binder[1], Alex Dayrit[1], Raul Ayala[2], Neil O'Brien[2], and Edward M. De Robertis[1*]

[1]Department of Biological Chemistry, David Geffen School of Medicine, University of California, Los Angeles, 90095-1662, USA

[2]Department of Medicine, David Geffen School of Medicine at UCLA

[3]These authors contributed equally

[*]Correspondence: ntejedamunoz@mednet.ucla.edu; ederobertis@mednet.ucla.edu

Tel. (310) 206-1401

SUMMARY

Activation of the Wnt pathway lies at the core of many human cancers. Interestingly, Wnt, cell adhesion, and macropinocytosis are often active in the same processes, and understanding how Wnt signaling and membrane trafficking cooperate should improve our understanding of embryonic development and cancer. Here we show that a macropinocytosis activator, the tumor promoter Phorbol 12-myristate 13-acetate (PMA), enhances Wnt signaling. Experiments using the *Xenopus* embryo as an in vivo model showed marked cooperation between the PMA phorbol ester and Wnt signaling, which was blocked by inhibitors of macropinocytosis, Rac1 activity, and lysosome acidification. The crosstalk between canonical Wnt, the Protein Kinase C (PKC) pathway, focal adhesions, lysosomes, and macropinocytosis suggests possible therapeutic targets for cancer progression in Wnt-driven cancers.

KEYWORDS

Wnt signaling, PMA, lysosome, colorectal carcinoma, multivesicular bodies, macropinocytosis, membrane trafficking, Focal Adhesion Kinase

INTRODUCTION

Cancer progression is a process during which mutations in various signaling pathways accumulate in the cell leading to uncontrolled growth (Kinzler and Vogelstein, 1996; Hanahan and Weinberg, 2011). Cancer progression is also influenced by tumor promoters, substances that do not mutate the DNA by themselves but nevertheless facilitate cancer development. In 1941 I. Berenblum and Peyton Rous found that inflammatory agents such as croton oil or turpentine could induce skin cancer when applied repeatedly to mouse or rabbit skin, but only when an initiator mutagen such as benzopyrene or anthracene had been previously painted on that patch of skin (Berenblum, 1941; Rous and Kidd, 1941). The active agent in croton oil was later purified and found to be the phorbol ester Phorbol-12-myristate-13-acetate (PMA), also known as 12-O-tetradecanoylphorbol-13-acetate (TPA). The molecular mechanism by which PMA promotes cancer is incompletely understood but involves the activation of Protein Kinase C (PKC) in the plasma membrane, where PMA mimics the endogenous second messenger Diacylglycerol (DAG) (Nishizuka, 1984). Tumor promoters cause chronic inflammation and significantly contribute to tumorigenesis (Weinberg, 2007).

The canonical Wnt/β-catenin pathway is a major driver of cancer and plays a crucial role in embryonic development (MacDonald et al., 2009; Nusse and Clevers, 2017). In the case of colon cancer, the great majority of tumors are initiated by mutation of the tumor suppressor Adenomatous Polyposis Coli (APC), which is a component of the destruction complex that normally degrades the transcriptional regulator β-catenin, leading to its accumulation in the nucleus and benign polyp formation (Kinzler and Vogelstein, 1996; Segditsas and Tomlinson, 2006). Activation of the Wnt/β-catenin pathway is also the driving force in many other cancers (Galluzzi et al., 2019). A key regulator of Wnt signaling is Glycogen Synthetase 3 (GSK3), which

phosphorylates β-catenin, leading to the formation of a phosphodegron that triggers its degradation in the proteasome. Upon activation of the Wnt receptors, GSK3, together with the destruction complex, is sequestered into multivesicular bodies (MVBs), also known as the late endosomes (Taelman et al., 2010; Vinyoles et al., 2014). The translocation of GSK3 from the cytosol into MVBs/lysosomes leads to the stabilization of many other cellular proteins in addition to β-catenin, in a process designated Wnt-STOP (Wnt-Stabilization of Proteins) (Acebron et al., 2014; Albrecht et al., 2021).

The many GSK3 phosphorylation targets stabilized by Wnt signaling include regulators of macropinocytosis such as Ras, Rac1, and Pak1 (Taelman et al., 2010; Albrecht et al., 2020; Jeong et al., 2012). A recent advance was the realization that Wnt signaling requires macropinocytosis (i.e., cell drinking) in order to traffic activated Wnt receptors and GSK3 to MVBs and lysosomes (Redelman-Sidi et al., 2018; Tejeda-Muñoz et al., 2019). Wnt-induced macropinocytosis also causes the internalization of focal adhesions and integrins from the cell surface into MVBs (Tejeda et al., 2022). The requirement of macropinocytosis for Wnt signaling is revealed, for example, by the decrease in nuclear β-catenin when colorectal cancer (CRC) cells mutant for APC were treated with macropinocytosis inhibitors such as the derivative of the diuretic Amiloride known as 5-(N-Ethyl-N-isopropyl) Amiloride (EIPA) (Tejeda-Muñoz et al., 2019; Tejeda-Muñoz and De Robertis, 2022a, 2022b;). Macropinocytosis is emerging in the field as a promising target for cancer treatment (Lambies and Commisso, 2022). In addition, it has been found that the macropinocytosis induced by Wnt signaling causes significant lysosome acidification and activation (Albrecht et al., 2020). There is also accumulating evidence showing that the size and number of lysosomes increase during carcinogenesis (Cardone et al., 2005; Kroemer and Jäättelä, 2005; Zhitomirsky and Assaraf, 2016). Lysosomes, previously thought to be the garbage disposal

of the cell, have emerged as central organelles in cancer (Kallunki et al., 2012; Kirkegaard and Jäättelä, 2009).

From the considerations above, investigating the intersection of Wnt signaling, macropinocytosis, lysosomes, focal adhesions, and membrane trafficking, is of great interest. While in most cells macropinocytosis requires stimulation of receptor tyrosine kinase (RTK) (Haigler et al., 1979; Yoshida et al., 2018), Ras (Bar-Sagi and Feramisco 1986; Commisso, 2013), or Wnt (Redelman-Sidi et al., 2018; Tejeda et al., 2019), some cells, such as amoebae and macrophages, as have constitutive macropinocytosis. Importantly, Swanson discovered that the phorbol ester PMA stimulated macropinocytosis even in macrophages that were thought to have fully activated constitutive macropinocytosis (Swanson, 1989).

In the present study, we asked whether phorbol ester could interact with canonical Wnt signaling. Using the *Xenopus* embryo, which provides a premier model system to analyze the Wnt pathway, we found that PMA, which lacked any effects on its own, greatly sensitized the embryo to dorsalization by Wnt signaling, leading to the formation of radial head structures lacking trunks. The dorsalizing effect of PMA on embryos was blocked by the macropinocytosis inhibitor EIPA, the Rac1 inhibitor EHT1864 (an upstream regulator of an upstream regulator of p21-activated kinase 1, Pak1, which is required for actin-mediated macropinocytosis), and the lysosomal V-ATPase inhibitor Bafilomycin A (Baf). Lysosomal activity was specifically required at the 32-cell stage for the activity of the Wnt-mimicking GSK3 inhibitor Lithium Chloride (LiCl). Ectopic axes induced by dominant-negative GSK3 (DN-GSK3-β) or β-catenin mRNAs were blocked by EIPA or Dominant-negative Rab7, indicating a widespread requirement of membrane trafficking for Wnt signaling. This involvement of membrane trafficking in Wnt-driven cancer was supported by immunostaining results of arrayed human CRC histological sections, in which we found that the

grade of malignancy increased Pak1, CD63 (an MVB marker), and V0a3 (a V-ATPase subunit that marks lysosomes) levels, while decreasing GSK3. In *Xenopus* embryos, twinning induced by Xwnt8 mRNA microinjection was blocked by inhibition of Rac1. In cultured CRC SW480 cells reconstituted with APC, the focal adhesion marker Tes was cytoplasmic, while the same cells mutant for APC (in which the Wnt pathway is activated) Tes and FAK (Focal Adhesion Kinase) were nuclear. The results suggest that macropinocytosis and membrane trafficking play an important role in embryogenesis and cancer progression.

RESULTS

The Phorbol Ester PMA Potentiates Wnt-like Signals in *Xenopus* embryos Via Macropinocytosis and Lysosomal Acidification.

Wnt is one of the earliest signals in the embryo and it induces the formation of the primary dorsal-ventral and head-to-tail axes, organogenesis, asymmetrical stem cell division, and regeneration (Loh et al., 2016; Niehrs, 2012). It is known that β-catenin is required for Wnt signaling activation on the dorsal side during early cleavage. Recently, we reported that inhibition of macropinocytosis with EIPA, or of lysosomal acidification with Baf, ventralized endogenous early dorsal axis formation, leading in particular to reduced head and brain structures (Tejeda-Munoz and De Robertis, 2022a). Activation of lysosomes on the dorsal side was detectable already at the 64-cell stage (Tejeda-Munoz and De Robertis, 2022a). To detect macropinocytosis directly, we now injected the macropinocytosis marker TMR-dextran 70kDa, which has a hydrated diameter of more than 200 nM and is diagnostic of large endocytic cups (Commisso et al., 2013, 2014).

We found that microinjection of TMR-dextran into the gastrula cavity showed stronger macropinocytosis just above the dorsal lip of the blastopore (Fig. 1A and B, indicated with an asterisk). While macropinocytosis probably also occurs at earlier stages, the blastocele cavity is not large enough during the cleavage stages to perform this microininjection experiment.

To test whether increasing macropinocytosis affected embryonic dorsal patterning, we used microinjections of PMA, which is known to increase macropinocytosis in macrophages (Swanson, 1989). We used a sensitized system in which a small amount of the GSK3 inhibitor Lithium chloride (LiCl) (4 nl at 300 mM in a single ventral injection at 4-cells) causes only a small dorsalization with slightly enlarged heads (Kao et al., 1986; Tejeda-Munoz and De Robertis, 2022a). The early Wnt signal can be detected at blastula (stage 9.5, just after the start of zygotic transcription) by measuring transcripts of the Wnt target genes *Siamois* and *Xnr3* by qRT-PCR (Tejeda-Munoz and De Robertis, 2022a). As shown in Figure 1C, PMA alone (4 nl at 500 nM) was without any effect, LiCl increased the Wnt target genes, and the combination of PMA and LiCl synergized significantly, elevating *Siamois* and *Xnr3* transcript levels.

The dorsalizing effects of PMA were most striking when phenotypes were analyzed at the early tailbud stage (Figure 1D-K). LiCl alone expanded head structures only slightly and PMA alone was without effect (Figures 1D, E, and H). However, the combination of PMA and LiCl lead to radially dorsalized embryos consisting of head structures lacking trunks (compare Figure 1E to 1I). This striking phenotype was eliminated by co-injection of EIPA or Baf, indicating that macropinocytosis and lysosomal acidification are required for the effects of PMA (Figure 1J and 1K). Injection of Baf alone decreased head and neural development, supporting a requirement for lysosomes for endogenous dorsal axis formation (Figure 1G). In target gene transcription assays, EIPA and Baf also blocked the increase in *Siamois* and *Xnr3* caused by PMA/LiCl (Figure 1C).

Using the BAR (β-catenin activity reporter) assay system (Biechele and Moon, 2008) in a cultured HEK293 permanent BAR/Renilla cell line, PMA synergized with LiCl when assayed both by β-catenin protein levels and BAR luciferase activity (Supplementary Figure S1). PMA alone caused a slight increase in β-catenin protein that lacked statistical significance (Figure S2C and S2I). This is presumably due to a small amount of endogenous Wnt secreted by this cell line (Colozza et al., 2020). However, PMA on its own had no detectable effect on BAR reporter activity (Figure S1J). Importantly, the effect of PMA on the activation of the Wnt pathway by GSK3 inhibition was abrogated by the inhibition of V-ATPase with Baf (Figure S1).

These results in embryos and cultured cells indicate that the tumor promoter PMA potentiates the Wnt signaling pathway and that this cooperation requires macropinocytosis and lysosomal acidification.

Lysosomal Activity is Required at the 32-cell Stage for Early Wnt Activation

In previous work, we had shown that immersion of embryos in the V-ATPase inhibitor Baf at 5 μM for only 7 minutes at the 32-cell stage resulted in macrocephalic embryos lacking cement glands (Tejeda-Muñoz and De Robertis, 2022a). To test whether this ventralization is caused by inhibition of the endogenous Wnt pathway signal, we now followed an initial Baf incubation with a second brief incubation in LiCl while still at the 32-cell stage. LiCl treatment has been shown to induce macropinocytosis in *Xenopus* embryos (Albrecht et al., 2020). It was found that ventralization by inhibiting V-ATPase was entirely rescued by the subsequent 7 minute pulse of LiCl, resulting in strongly dorsalized tadpoles with large heads (Figure 2A-D). These phenotypes correlate with the activation of Wnt signaling, as indicated by qRT-PCR of Wnt targets at the blastula stage (Figure 2E). In the converse experiment, when embryos were treated with LiCl,

washed, and then incubated for 7 minutes in Baf, the effect of lysosomal inhibition was dominant, resulting in ventralized tailbud embryos (Figure 2F-2J). This order-of-addition experiment strongly supports the proposal (Tejeda-Muñoz and De Robertis, 2022a) that lysosomal activity is required for the initial endogenous Wnt signal at the 32-cell stage of development.

Wnt Pathway Signaling in Microinjected Embryos or APC Mutant Cells Requires Macropinocytosis and Membrane Trafficking

Next, we tested the requirement for macropinocytosis of different components of the Wnt pathway using the axis duplication assay (McMahon and Moon, 1989). Microinjection of Wnt-mimic dominant-negative GSK3 (DN-GSK3-β) mRNA, a catalytically inactive form of GSK3, induced complete axis duplications, which were blocked by the co-injection of the macropinocytosis inhibitor EIPA (1 mM, 4 nl) (Figure 3A-D). Secondary axis induction by β-catenin mRNA was also abrogated by EIPA, as well as the membrane trafficking inhibitor dominant-negative Rab7 (DN-Rab7) (Figure 3E-H). β-catenin is a transcriptional activator, and one might have not expected a requirement for membrane trafficking. However, axis formation is a multistep process and appears to require macropinocytosis and Rab7 activity in addition to transcriptional activation of Wnt target genes.

Macropinocytosis is an actin-driven process that is orchestrated by Pak1 kinase, which in turn is activated by Rac1. Rac1 activity is essential for the formation of lamellipodia and macropinocytic cups (Hall, 1998). EHT1864 (EHT) is a specific inhibitor of Rac1 that has the practical advantage of being water-soluble (Hampsch et al., 2017). When embryos were immersed in EHT at the critical 32-cell stage for 7 minutes (10 mM), head structures were greatly reduced, and ventral posterior structures expanded (Figures 4A and 4B). This was accompanied by a

significant increase of transcripts of the ventral markers Sizzled and Vent1 at the blastula stage (Figure 4C).

Microinjection of a small amount of EHT (1 mM, 4 nl, 1x ventral at 4-cell) was without effect on its own but was able to block the axis-duplication effect of microinjecting Wnt8 mRNA (Figure 4D-G). Quantitative RT-PCR analyses at the blastula stage confirmed that inhibiting Rac1 inhibited the induction of *Siamois* and *Xnr3* caused by xWnt8 mRNA microinjection (Figure 4H). In SW480 CRC cells, which have constitutively activated Wnt due to mutation of APC (Leibovitz et al., 1976; Faux et al., 2004), EHT inhibited the size of cell spheroids in hanging drop cultures (Figure S2A-C) and, importantly, significantly inhibited macropinocytosis uptake of TMR-dextran in these cancer cells (Figure S2D-F). SW480 cells have high constitutive nuclear β-catenin and Rac1 plasma membrane levels (Figure 4I-I''). After overnight treatment with the macropinocytosis inhibitor EIPA, both proteins decreased greatly, indicating a requirement of sustained macropinocytosis for the stability of these proteins (Figure 4J-J'').

The results show that signaling by Wnt/β-catenin requires macropinocytosis, Rac1, and membrane trafficking in *Xenopus* embryos and in cancer cells with constitutive Wnt signaling.

Tumor Progression in Human Colorectal Cancers Correlates with a Role for membrane Trafficking in Wnt/β-catenin Signaling

Colorectal cancer is particularly favorable for the analysis of tumor progression because it gradually accumulates mutations, and in over 85% of the cases the initial driver mutation is in the APC tumor suppressor (Kinzler and Volgelstein, 1996; Weinberg, 2007). This offered an opportunity to test our proposal that membrane trafficking and its molecular components play an important role in Wnt-driven cancers (Albrecht et al., 2021; Tejeda-Muñoz and De Robertis,

2022b). Commercially available arrays of paraffin-sectioned histological sections containing 90 cases of adenocarcinoma of various grades I-IV and 90 samples of corresponding adjacent normal tissues (from TissueArray) were used for immunostaining. Arrays were double stained for β-catenin and antibodies against proteins involved in the macropinocytosis/MVB/lysosome/GSK3 pathway. Each individual section was evaluated, and normal colon, adenocarcinoma I, and adenocarcinoma IV were compared to assess the predominant effect of cancer progression.

As shown in Figure 5, β-catenin levels consistently correlated with grade IV malignancy when compared to normal colon or grade I cancers. Pak1, a kinase required for macropinocytosis and Wnt signaling (Redelman-Sidi et al., 2018; Albrecht et al.,2020) was significantly elevated with increased malignancy (Figure 5A-C''). CD63, a tetraspan protein that marks MVB intraluminal vesicles (Escola et al., 1998), reached high levels in adenocarcinoma IV (Figure 5D-F''), particularly in cells with the highest β-catenin expression (compare Figure 5F to 5F'). This increase in MVBs is in agreement with the GSK3 sequestration model of Wnt signaling (Taelman et al., 2010). The V-ATPase subunit V0a3, a marker for acidic lysosomes (Ramirez et al., 2019), also increased strongly with the CRC malignancy (compare Figure 5G to 5I). The cellular levels of total GSK3 decreased with malignancy (Figure 5J-L'', compare 5J to 5L), as predicted by the sequestration model (Taelman et al., 2010). During Wnt signaling, GSK3 is sequestered into MVBs which are trafficked into lysosomes and a decrease was to be expected after sustained Wnt activation. Previously, we had been unable to demonstrate a decrease in total cellular GSK3 levels during acute Wnt signaling experiments (Taelman et al., 2010). The co-localization of β-catenin with Pak1, CD63, V0a3, or GSK3 in human colorectal adenocarcinomas was quantified in Figures S3A-S3D.

These results were confirmed by examining immunostaining levels of Pak1, V0a3, and GSK3 compared to β-catenin protein in mouse xenografts in a CD1 NU/NU nude mouse model injected with SW480 human CRC cells (in which Wnt activation is known to be caused by APC mutation, Faux et al., 2004). In this case, tumor cells were compared to normal colon mouse tissue sections. The results showed that CRC cells had high levels of β-catenin, Pak1, and lysosomes, while GSK3 levels were reduced (Figure S3E-M), in agreement with the results in human tissue arrays.

These in vivo observations in human tumors are consistent with the view that macropinocytosis components, MVBs, and lysosomes increase with CRC malignancy. Further, the decrease in total GSK3 levels suggests a role in the trafficking and degradation of this key enzyme in cancer.

Wnt Affects the Subcellular Localization of Focal Adhesion Components

Previous work from our lab showed that Wnt treatment rapidly induces the endocytosis of multiple focal adhesion (FA) proteins, including integrin β-1 (ITGβ-1), from the cell surface (Tejeda-Muñoz et al., 2022). FAs link the actin cytoskeleton with the extracellular matrix (Figure 6A). Some focal adhesion proteins shuttle between the nucleus, cytoplasm and focal adhesion sites, and are proposed to play a role in cancer (Nix and Beckerle, 1997). FA components containing LIM domains can shuttle between the nucleus and cytoplasm (Kadrmas and Beckerle, 2004; Anderson et al., 2021). We now investigated whether constitutive Wnt signaling regulates FAs trafficking using the SW480 and SW480APC system, in which the stable reconstitution with full-length APC restores these CRC cells to a non-malignant phenotype (Faux et al., 2004), which is accompanied by a decrease in β-catenin levels (Figure 6B). As shown in Figure 6C to 6D'', the PET-LIM domain

FA protein Tes (also known as Testin) (Garvalov et al., 2003) was cytoplasmic in SW480APC, but was nuclear in SW480 cells in which Wnt is activated by APC mutation. The nuclear localization of Tes in SW480 cells required macropinocytosis, since treatment with EIPA resulted in its re-localization to the cytoplasm (Figure 4E-4F''). This result was consistent with the idea that membrane trafficking is required for constitutive Wnt signaling in cancer (Tejeda-Muñoz et al., 2019). In the nude mouse xenograft model, Tes was abundant in the cytoplasm of the normal colon, while in SW480 it localized in the nucleus of those cells with the highest β-catenin levels (Figure 6G-6I''). The function of TES is poorly understood, but it has been proposed to act as a tumor suppressor (Tatarelli et al., 2000; Tobias et al., 2001); the present results suggest that Tes may serve as a Wnt-regulated nuclear marker in CRC.

Focal Adhesion Kinase (FAK) is a key regulator of FA maintenance and signaling, known to interact with the Wnt pathway in various ways (Chuang et al., 2022). In HEK293 BAR/Renilla cells treatment with FAK inhibitor PF-00562271 strongly decreased β-catenin signaling by LiCl inhibition of GSK3 (Figure 6J). In SW480 cells, FAK had nuclear and cytoplasmic localization (Figure 6A-A''). Overnight treatment with FAK inhibitor PF-00562271 resulted in the reduction of β-catenin and of FAK itself (Figure S4B-B''). Importantly, the addition of the tumor promoter PMA to SW480 cells (in which the Wnt pathway is constitutively activated) strongly increased protein levels of β-catenin and FAK protein (Figure 6K-6L''). The effect of PMA was abrogated by EIPA or Baf treatment (Figure S4C-S4H''), indicating that the increase in FAK levels requires macropinocytosis and lysosome activity.

The shuttling of FA components between cytoplasm and nucleus when Wnt signaling is activated by APC mutation, and increased by the macropinocytosis-inducing tumor promoter

PMA, is probably just the tip of the iceberg of the role of membrane trafficking in Wnt-driven cancers.

DISCUSSION

The present work was inspired by the discovery that PMA increases macropinocytosis (Swanson, 1989). Our experiments support the role of membrane trafficking in canonical Wnt signaling in embryos and cancer cells and are summarized in the model in Figure 7. The main finding was a synergistic effect between the tumor promoter phorbol ester (PMA) and activation of the Wnt/β-catenin pathway that was blocked by EIPA or Baf (Figure 1). EIPA is a macropinocytosis inhibitor of the Na^+/H^+ exchanger at the plasma membrane; it causes acidification of the submembranous cytoplasm and prevents actin polymerization (Koivusalo et al., 2010). Bafilomycin A (Baf) is an inhibitor of the V-ATPase that drives membrane trafficking and lysosomal acidification. PMA plays an important role in our understanding of tumor biology because it is the archetypal tumor promoter, able to promote tumor growth without further mutation of the DNA (Berenblum, 1941; Weinberg, 2007). PMA activates the PKC pathway (Takai et al., 1979; Nishizuka, 1984), and there is previous literature on the crosstalk between the PKC and Wnt pathways (Schwarz et al., 2013; Goode et al., 1992). What is novel in the present paper is the connection between macropinocytosis, membrane trafficking, lysosomes, focal adhesions, PMA, and Wnt signaling.

Macropinocytosis, Rac1, and Wnt signaling

Wnt signaling triggers lysosomal acidification in addition to macropinocytosis (Albrecht et al., 2020). Baf blocks the synergy between PMA and the Wnt-mimic LiCl in embryos microinjections.

It also blocks development of the endogenous axis, particularly the head region when embryos are briefly immersed in Baf at the 32-cell stage (Tejeda-Muñoz and De Robertis, 2022). Using order-of-addition experiments in which embryos were briefly treated with pulses of Baf or the GSK3 inhibitor LiCl, we showed that the requirement for lysosome acidification was due to inhibition of the Wnt pathway at the 32-cell stage (Figure 2). Co-injection experiments of DN-GSK3 or β-catenin mRNAs with DN-Rab7 or EIPA supported the view that membrane trafficking and macropinocytosis are essential for the induction of secondary axes in *Xenopus* (Figure 3).

Rac1 is an upstream regulator of the Pak1 kinase required for macropinocytosis (Redelman-Sidi et al., 2018). Rac1 is a member of the family of small Rho GTPases that drives the formation of lamellipodia, membrane ruffles, and macropinocytosis (Hall, 1998; Egami et al., 2014; Fujii et al., 2013). The Rac1 inhibitor EHT1864 (Hampsch et al., 2017) strongly ventralized the endogenous axis of embryos after brief incubation at the critical 32-cell stage. In co-injection experiments EHT blocked the axis-inducing effect of microinjected xWnt8 mRNA (Figure 4). Rac1 is a regulator of multiple signaling cascades and has been reported to increase the nuclear translocation of β-catenin (Wu et al., 2008). Other work showed that Rac1 binds to β-catenin and promotes the formation of nuclear β-catenin/LEF1 complexes (Jamieson et al., 2015). In the context of the present study, Rac1 levels were decreased by treating CRC cells with EIPA, and Rac1 inhibition blocked Wnt signaling in embryos, indicating that Rac1 may crosstalk with Wnt through macropinocytosis.

Lysosomes, cancer and focal adhesions

The lysosome is considered a promising target for the treatment of cancer (Fehrenbacher and Jäättelä, 2005; Lawrence and Zoncu, 2019). We used human CRC tissue arrays to analyze whether

lysosomes and membrane trafficking correlate with cancer progression. Most colorectal tumors are initiated by mutation of APC, which drives Wnt signaling (Kinzler and Vogelstein, 1996; Segditsas and Tomlinson, 2006). It was found that advanced grades of colon carcinoma correlated with increase immunostaining for Pak1 (driver of macropinocytosis), CD63 (MVB/late endosome marker), and V0a3 (lysosomal V-ATPase marker) (Figure 5). In addition, cancer malignancy correlated with low levels of GSK3 staining, both in human samples and nude mouse SW480 xenografts. Previous literature points to the physiological relevance of lysosomes during cancer. Cancer cells require lysosome function and have changes in lysosomal volume and subcellular localization during oncogenic transformation (Kallunki et al., 2012; Kirkegaard and Jäättelä, 2009; Gocheva and Joyce, 2007; Kolwijck et al., 2010). Lysosome-associated membrane protein 1 (LAMP-1) has been reported on the cell surface of highly metastatic colon cells (Ranjbar and Jamshidi, 2022) and V-ATPase has been associated with extracellular acidification and cancer cell invasion (Capecci and Forgac, 2013; Hinton et al., 2009; Perona and Serrano, 1988). The results reported here support the view (Taelman et al., 2010; Tejeda-Muñoz and De Robertis, 2022) that Wnt-driven lysosomal acidification and GSK3 sequestration may play a role in cancer. In addition, MVB/lysosome components could serve as markers for advanced Wnt-driven cancers.

The cytoskeleton interacts with proteins of the extracellular matrix though focal adhesions (Geiger et al., 2001). We have previously reported that Wnt causes the endocytosis of FA proteins and depletion of Integrin β-1 from the cell surface (Tejeda-Muñoz et al., 2022). We now report that Tes, a member of the PET-LIM family of focal adhesion proteins, changed subcellular localization after Wnt activation in SW480 cells. It is known that other focal adhesions shuttle between the nucleus, cytoplasm, and focal adhesion sites and may play important roles in cancer (Chaturvedi et al., 2012; Nix and Beckerle, 1997). FAK is a key signaling kinase that regulates

focal adhesion signaling. In SW480 cells, which have constitutive Wnt signaling, FAK protein was increased by PMA, and this was inhibited by EIPA or Baf (Figure 6). These results suggest that the crosstalk between focal adhesions and Wnt signaling could be relevant in cancer progression.

Cooperation between PMA and Wnt

PMA activates PKC signaling by mimicking its physiological second messenger diacylglycerol (DAG), an activator of protein kinase C. There is previous literature implicating PKC isozymes in the regulation of the Wnt signaling pathway (Fang et al., 2002; Goode et al., 1992) and that different PKC isoforms can have positive or negative effects on Wnt/β-catenin signaling (Ohno and Nishizuka, 2002). However, the molecular role of PKC isoforms in the Wnt signaling pathway remains poorly understood (Bhatia and Spiegelman, 2005; Schwarz et al., 2013) It has been reported that PMA can stabilize CK1ε (Casein Kinase 1 epsilon), enhance its kinase activity, and induce LRP6 phosphorylation at Thr1479 and Ser1490, leading to the activation of the Wnt/β-catenin pathway (Su et al., 2018).

In the context of the present study, it is relevant that Wnt signaling rapidly triggers macropinocytosis and trafficking into lysosomes (Tejeda-Muñoz et al., 2019). Macropinocytosis requires the activation of Phosphoinositide 3 Kinase (PI3K) which leads to the formation of patches of PIP_3 in the inner plasma membrane leaflet that initiate the formation of macropinocytic cups (Egami et al., 2014; Yoshida et al., 2018). During macropinosome formation, the PIP_3 lipid is then converted into DAG by Phospholipase C gamma 1 (PLCγ1), and DAG activates PKC signaling (Yoshida et al., 2018). It seems possible that PMA may facilitate Wnt/β-catenin signaling by mimicking the DAG concentrated in macropinosomes. A future test for this hypothesis will be

to directly add DAG to cells and follow its effects on Wnt/β-catenin signaling. In addition, it will be interesting to study the role of chronic inflammation on macropinocytosis and tumor promotion. Active PKC phosphorylates many targets, including IκB Kinase (IKK) which becomes activated and phosphorylates Inhibitor of NF-κB (IκB), targeting it for degradation and triggering inflammation (Weinberg, 2007). Tumor progression is promoted by many chronic inflammatory agents such as turpentine, distilled alcoholic beverages, hepatitis viruses, and *Helicobacter pylori* that do not cause mutations by themselves but regulate the expansion of previously mutant clones (Rous and Kidd, 1941; Weinberg, 2007). Taken together, the results presented here suggest that macropinocytosis, lysosomal activity, and membrane trafficking are possible therapeutic targets for tumor progression in Wnt-driven cancers.

STAR★METHODS

Detailed methods are provided in the online version of this paper and include the following:

KEY RESOURCES TABLE

RESOURCE AVAILABILITY

Lead contact

Materials availability

Data and code availability

EXPERIMENTAL MODEL AND SUBJECT DETAILS

Tissue culture and transfection

Xenopus embryo microinjection

Bisected embryo TMR-dextran staining

Human colon cancer tissue array and immunochemistry

Xenograft tumor model

Antibodies and reagents

METHOD DETAILS

Immunostainings

Western blots

Luciferase assay

3D spheroid cell culture

Bafilomycin treatments in *Xenopus* embryos

LiCl and Bafilomycin sequential treatments

qRT-PCR

QUANTIFICATION AND STATISTICAL ANALYSIS

SUPPLEMENTAL INFORMATION

Supplemental information can be found online at ….

ACKNOWLEDGEMENTS

We are grateful to Yi Ding and Yuki Moriyama for comments on the manuscript. We are grateful for funding to the UC Cancer Research Coordinating Committee (grant C21CR2039); National Institutes of Health grant P20CA016042 to the University of California, Los Angeles Jonsson Comprehensive Cancer Center; and the Norman Sprague Endowment for Molecular Oncology.

AUTHOR CONTRIBUTIONS

N.T.-M. and E.M.D.R designed the research; N.T.-M. and E.M.D.R. wrote the manuscript. N.T.-M., Y.A., J.M., G.B., N.O., R. A., and E.D.R. performed research. All authors reviewed the published version of the manuscript.

DECLARATION OF INTERESTS

The authors declare no competing interests.

REFERENCES

Acebron, S. P., Karaulanov, E., Berger, B. S., Huang, Y.-L., and Niehrs, C. (2014). Mitotic Wnt signaling promotes protein stabilization and regulates cell size. Mol. Cell *54*, 663–674. https://doi.org/10.1016/j.molcel.2014.04.014.

Albrecht, L. V., Tejeda-Muñoz, N., and De Robertis, E. M. (2021). Cell biology of canonical Wnt signaling. Ann. Rev. Cell Dev. Biol. *37*, 369–389. https://doi.org/10.1146/annurev-cellbio-120319-023657.

Albrecht, L. V., Tejeda-Muñoz, N., Bui, M. H., Cicchetto, A. C., Di Biagio, D., Colozza, G., Schmid, E., Piccolo, S., Christofk, H. R., and De Robertis, E. M. (2020). GSK3 inhibits macropinocytosis and lysosomal activity through the Wnt Destruction Complex Machinery. Cell Rep. *32*, 107973. https://doi.org/10.1016/j.celrep.2020.107973.

Anderson, C. A., Kovar, D. R., Gardel, M. L., and Winkelman, J. D. (2021). LIM domain proteins in cell mechanobiology. Cytoskeleton *78*, 303–311. https://doi.org/10.1002/cm.21677.

Bar-Sagi, D. and Feramisco, J. R. (1986). Induction of membrane ruffling and fluid-phase pinocytosis in quiescent fibroblasts by ras proteins. Science *233*, 1061–1068. https://doi.org/10.1126/science.3090687.

Berenblum, I. (1941). The cocarcinogenic action of croton resin. Cancer Res., 1, 44-48.

Bhatia, N. and Spiegelman, V. S. (2005). Activation of wnt/beta-catenin/TCF signaling in mouse skin carcinogenesis. Mol. Carcinog. *42*, 213–221. https://doi.org/10.1002/mc.20077.

Biechele, T. L., and Moon, R. T. (2008). Assaying beta-catenin/TCF transcription with beta-catenin/TCF transcription-based reporter constructs. Methods Mol. Biol., *468*, 99–110. https://doi.org/10.1007/978-1-59745-249-6_8.

Capecci, J. and Forgac, M. (2013). The function of vacuolar atpase (V-atpase) subunit isoforms in invasiveness of MCF10a and mcf10ca1a human breast cancer cells. J. Biol. Chem. *288*, 32731–32741. https://doi.org/10.1074/jbc.m113.503771.

Cardone, R. A., Casavola, V., and Reshkin, S. J. (2005). The role of disturbed pH dynamics and the Na+/H+ exchanger in metastasis. Nat. Rev. Cancer *5*, 786–795. https://doi.org/10.1038/nrc1713.

Chaturvedi, A., Hoffman, L. M., Welm, A. L., Lessnick, S. L., and Beckerle, M. C. (2012). The EWS/FLI oncogene drives changes in cellular morphology, adhesion, and migration in Ewing Sarcoma. Genes Cancer, *3*, 102–116. https://doi.org/10.1177/1947601912457024.

Chuang H.H., Zhen Y.Y., Tsai Y.C., Chuang C.H., Hsiao M., Huang M.S., Yang C.J. (2022). FAK in cancer: from mechanisms to therapeutic strategies. Int. J. Mol. Sci., *23*, 1726. https://doi.org/10.3390/ijms23031726.

Colozza, G., and De Robertis, E. M. (2014). Maternal syntabulin is required for dorsal axis formation and is a germ plasm component in xenopus. Differentiation, *88*, 17–26. https://doi.org/10.1016/j.diff.2014.03.002.

Colozza, G., Jami-Alahmadi, Y., Dsouza, A., Tejeda-Muñoz, N., Albrecht, L. V., Sosa, E. A., Wohlschlegel, J. A., and De Robertis, E. M. (2020). Wnt-inducible LRP6-APEX2 interacting proteins identify escrt machinery and trk-fused gene as components of the Wnt Signaling Pathway. Sci. Rep., *10,* 21555. https://doi.org/10.1038/s41598-020-78019-5.

Commisso, C., Davidson, S. M., Soydaner-Azeloglu, R. G., Parker, S. J., Kamphorst, J. J., Hackett, S., Grabocka, E., Nofal, M., Drebin, J. A., Thompson, C. B., et al. (2013). Macropinocytosis of protein is an amino acid supply route in Ras-transformed cells. Nature, *497*, 633–637. https://doi.org/10.1038/nature12138.

Commisso, C., Flinn, R. J., and Bar-Sagi, D. (2014). Determining the macropinocytic index of cells through a quantitative image-based assay. Nat. Protoc., *9*, 182–192. https://doi.org/10.1038/nprot.2014.004.

Egami, Y., Taguchi, T., Maekawa, M., Arai, H., and Araki, N. (2014). Small GTPases and phosphoinositides in the regulatory mechanisms of macropinosome formation and maturation. Front. Physiol., *5*. https://doi.org/10.3389/fphys.2014.00374.

Escola, J.-M., Kleijmeer, M. J., Stoorvogel, W., Griffith, J. M., Yoshie, O., and Geuze, H. J. (1998). Selective enrichment of tetraspan proteins on the internal vesicles of multivesicular endosomes and on exosomes secreted by human B-lymphocytes. J. Biol. Chem., *273*, 20121–20127. https://doi.org/10.1074/jbc.273.32.20121.

Fang, X., Yu, S., Tanyi, J. L., Lu, Y., Woodgett, J. R., and Mills, G. B. (2002). Convergence of multiple signaling cascades at glycogen synthase kinase 3: EDG receptor-mediated phosphorylation and inactivation by lysophosphatidic acid through a protein kinase C-dependent intracellular pathway. Mol. Cell. Biol., *22*, 2099–2110. https://doi.org/10.1128/mcb.22.7.2099-2110.2002.

Faux, M. C., Ross, J. L., Meeker, C., Johns, T., Ji, H., Simpson, R. J., Layton, M. J., and Burgess, A. W. (2004). Restoration of full-length adenomatous polyposis coli (APC) protein in a colon cancer cell line enhances cell adhesion. J. Cell. Sci., *117*, 427–439. https://doi.org/10.1242/jcs.00862.

Fehrenbacher, N., and Jäättelä Marja. (2005). Lysosomes as targets for cancer therapy. Cancer Res., *65*, 2993–2995. https://doi.org/10.1158/0008-5472.can-05-0476.

Fujii, M., Kawai, K., Egami, Y., and Araki, N. (2013). Dissecting the roles of RAC1 activation and deactivation in macropinocytosis using microscopic photo-manipulation. Sci. Rep., *3*. https://doi.org/10.1038/srep0238.5.

Galluzzi, L., Spranger, S., Fuchs, E., and López-Soto, A. (2019). Wnt signaling in Cancer Immunosurveillance. Trends Cell Biol., *29*, 44–65. https://doi.org/10.1016/j.tcb.2018.08.005.

Gao, C., Chen, G., Kuan, S.-F., Zhang, D. H., Schlaepfer, D. D., and Hu, J. (2015). FAK/Pyk2 promotes the Wnt/β-catenin pathway and intestinal tumorigenesis by phosphorylating GSK3β. eLife, *4*. https://doi.org/10.7554/elife.10072.

Garvalov, B. K., Higgins, T. E., Sutherland, J. D., Zettl, M., Scaplehorn, N., Köcher Thomas, Piddini, E., Griffiths, G., and Way, M. (2003). The conformational state of TES regulates its zyxin-dependent recruitment to focal adhesions. J. Cell. Biol., *161*, 33–39. https://doi.org/10.1083/jcb.200211015.

Geiger, B., Bershadsky, A., Pankov, R., and Yamada, K. M. (2001). Transmembrane crosstalk between the extracellular matrix and the cytoskeleton. Nat. Rev. Mol. Cell. Biol., *2*, 793–805. https://doi.org/10.1038/35099066.

Gocheva, V., and Joyce, J. A. (2007). Cysteine cathepsins and the cutting edge of cancer invasion. Cell Cycle, *6*, 60–64. https://doi.org/10.4161/cc.6.1.3669.

Goode, N., Hughes, K., Woodgett, J. R., and Parker, P. J. (1992). Differential regulation of glycogen synthase kinase-3 beta by protein kinase C isotypes. J. Biol. Chem., *267*, 16878–16882. https://doi.org/10.1016/s0021-9258(18)41866-2.

Griffith, E., Coutts, A. S., and Black, D. M. (2005). RNAi knockdown of the focal adhesion protein TES reveals its role in actin stress fibre organization. Cell Motil. Cytoskelet., *60*, 140–152. https://doi.org/10.1002/cm.20052.

Haigler, H. T., McKanna, J. A., and Cohen, S. (1979). Rapid stimulation of pinocytosis in human carcinoma cells A-431 by epidermal growth factor. J. Cell. Biol., *83*, 82–90. https://doi.org/10.1083/jcb.83.1.82.

Hall, A. (1998). Rho GTPases and the actin cytoskeleton. Science, *279*, 509–514. https://doi.org/10.1126/science.279.5350.509.

Hampsch, R. A., Shee, K., Bates, D., Lewis, L. D., Désiré, L., Leblond, B., Demidenko, E., Stefan, K., Huang, Y. H., and Miller, T. W. (2017). Therapeutic sensitivity to Rac GTPase inhibition requires consequential suppression of mTORC1, AKT, and MEK signaling in breast cancer. Oncotarget, *8*, 21806–21817. https://doi.org/10.18632/oncotarget.15586.

Hanahan, D., and Weinberg, R. A. (2011). Hallmarks of cancer: The next generation. Cell, *144*, 646–674. https://doi.org/10.1016/j.cell.2011.02.013.

Hinton, A., Sennoune, S. R., Bond, S., Fang, M., Reuveni, M., Sahagian, G. G., Jay, D., Martinez-Zaguilan, R., and Forgac, M. (2009). Function of a subunit isoforms of the V-atpase in pH homeostasis and in vitro invasion of MDA-MB231 human breast cancer cells. J. Biol. Chem., *284*, 16400–16408. https://doi.org/10.1074/jbc.m901201200.

Jamieson, C., Lui, C., Brocardo, M. G., Martino-Echarri, E., and Henderson, B. R. (2015). RAC1 augments Wnt signaling by stimulating β-catenin-LEF-1 complex assembly independent of β-catenin nuclear import. J. Cell. Sci. *128*, 3933–3946. https://doi.org/10.1242/jcs.167742.

Jeong, W.-J., Yoon, J., Park, J.-C., Lee, S.-H., Lee, S.-H., Kaduwal, S., Kim, H., Yoon, J.-B., and Choi, K.-Y. (2012). Ras stabilization through aberrant activation of Wnt/β-catenin signaling promotes intestinal tumorigenesis. Sci. Signal., *5*, ra30. https://doi.org/10.1126/scisignal.2002242.

Kadrmas, J. L., and Beckerle, M. C. (2004). The LIM domain: From the cytoskeleton to the nucleus. Nat. Rev. Mol. Cell. Biol., *5*, 920–931. https://doi.org/10.1038/nrm1499.

Kallunki, T., Olsen, O. D., and Jäättelä, M. (2012). Cancer-associated lysosomal changes: Friends or foes? Oncogene, *32*, 1995–2004. https://doi.org/10.1038/onc.2012.292.

Kao, K. R., Masui, Y., and Elinson, R. P. (1986). Lithium-induced respecification of pattern in xenopus laevis embryos. Nature, *322*, 371–373. https://doi.org/10.1038/322371a0.

Kinzler, K. W., and Vogelstein, B. (1996). Lessons from hereditary colorectal cancer. Cell, *87*, 159–170. https://doi.org/10.1016/s0092-8674(00)81333-1.

Kirkegaard, T., and Jäättelä, M. (2009). Lysosomal involvement in cell death and cancer. Biochem. Biophys. Acta - Mol. Cell Res., *1793*, 746–754. https://doi.org/10.1016/j.bbamcr.2008.09.008.

Koivusalo, M., Welch, C., Hayashi, H., Scott, C. C., Kim, M., Alexander, T., Touret, N., Hahn, K. M., and Grinstein, S. (2010). Amiloride inhibits macropinocytosis by lowering submembranous ph and preventing RAC1 and cdc42 signaling. J. Cell. Biol., *188*, 547–563. https://doi.org/10.1083/jcb.200908086.

Kolwijck, E., Massuger, L. F., Thomas, C. M., Span, P. N., Krasovec, M., Kos, J., and Sweep, F. C. (2010). Cathepsins B, l and cystatin C in cyst fluid of ovarian tumors. J. Cancer Res. Clin. Oncol., *136*, 771–778. https://doi.org/10.1007/s00432-009-0716-z.

Kroemer, G., and Jäättelä, M. (2005). Lysosomes and autophagy in cell death control. Nat. Rev. Cancer, *5*, 886–897. https://doi.org/10.1038/nrc1738.

Lambies, G., and Commisso, C. (2022). Macropinocytosis and cancer: From tumor stress to signaling pathways. Subcell. Biochem., *98*, 15–40. https://doi.org/10.1007/978-3-030-94004-1_2.

Lawrence, R. E., and Zoncu, R. (2019). The lysosome as a cellular centre for signalling, metabolism and quality control. Nat. Cell. Biol., *21*, 133–142. https://doi.org/10.1038/s41556-018-0244-7.

Leibovitz A., Stinson J.C., McCombs W.B. 3rd, McCoy C.E.., Mazur KC., Mabry N.D. (1976) Classification of human colorectal adenocarcinoma cell lines. Cancer Res. *36*, 4562-4569.

Loh, K. M., van Amerongen, R., and Nusse, R. (2016). Generating cellular diversity and spatial form: Wnt Signaling and the evolution of Multicellular Animals. Dev. Cell., *38*, 643–655. https://doi.org/10.1016/j.devcel.2016.08.011.

MacDonald, B. T., Tamai, K., and He, X. (2009). Wnt/β-catenin signaling: Components, mechanisms, and diseases. Dev. Cell., *17*, 9–26. https://doi.org/10.1016/j.devcel.2009.06.016.

McMahon, A. P., and Moon, R. T. (1989). Ectopic expression of the proto-oncogene int-1 in Xenopus embryos leads to duplication of the embryonic Axis. Cell, *58*, 1075–1084. https://doi.org/10.1016/0092-8674(89)90506-0.

Niehrs, C. (2012). The complex world of Wnt receptor signalling. Nat. Rev. Mol. Cell. Biol., *13*, 767–779. https://doi.org/10.1038/nrm3470.

Nishizuka, Y. (1984). The role of protein kinase C in cell surface signal transduction and tumour promotion. Nature, *308*, 693–698. https://doi.org/10.1038/308693a0.

Nix, D. A., and Beckerle, M. C. (1997). Nuclear–cytoplasmic shuttling of the focal contact protein, Zyxin: A potential mechanism for communication between sites of cell adhesion and the nucleus. J. Cell. Biol., *138*, 1139–1147. https://doi.org/10.1083/jcb.138.5.1139.

Nusse, R., and Clevers, H. (2017). Wnt/β-catenin signaling, disease, and emerging therapeutic modalities. Cell, *169*, 985–999. https://doi.org/10.1016/j.cell.2017.05.016.

Ohno, S., and Nishizuka, Y. (2002). Protein kinase C isotypes and their specific functions: prologue. J. Biochem., *132*, 509–511. https://doi.org/10.1093/oxfordjournals.jbchem.a003249.

Perona, R., and Serrano, R. (1988). Increased pH and tumorigenicity of fibroblasts expressing a yeast proton pump. Nature, *334*, 438–440. https://doi.org/10.1038/334438a0.

Ramirez, C., Hauser, A. D., Vucic, E. A., and Bar-Sagi, D. (2019). Plasma membrane V-atpase controls oncogenic Ras-induced macropinocytosis. Nature, *576*, 477–481. https://doi.org/10.1038/s41586-019-1831-x.

Ranjbar M.A. and Jamshidi M. (2022). Overexpression of Lysosome-Associated Membrane Protein 1 in Oral Squamous Cell Carcinoma and its Correlation with Tumor Differentiation

and Metastasis. Iran J Otorhinolaryngol. *34*, 3-8. https://doi.org/10.22038/IJORL.2021.51683.2772.

Redelman-Sidi, G., Binyamin, A., Gaeta, I., Palm, W., Thompson, C. B., Romesser, P. B., Lowe, S. W., Bagul, M., Doench, J. G., Root, D. E., et al. (2018). The canonical Wnt pathway drives macropinocytosis in cancer. Cancer Res., *78*, 4658–4670. https://doi.org/10.1158/0008-5472.can-17-3199.

Rous, P., and Kidd, J. G. (1941). Conditional neoplasms and subthreshold neoplastic states. A study of the tar tumors of rabbits. J. Exp. Med., *73*, 365–390. https://doi.org/10.1084/jem.73.3.365.

Schwarz, M., Münzel, P. A., and Braeuning, A. (2013). Non-melanoma skin cancer in mouse and man. Arch. Toxicol., *87*, 783–798. https://doi.org/10.1007/s00204-012-0998-9.

Segditsas, S., and Tomlinson, I. (2006). Colorectal cancer and genetic alterations in The wnt pathway. Oncogene, *25*, 7531–7537. https://doi.org/10.1038/sj.onc.1210059.

Su, Z., Song, J., Wang, Z., Zhou, L., Xia, Y., Yu, S., Sun, Q., Liu, S.-S., Zhao, L., Li, S., et al. (2018). Tumor promoter TPA activates Wnt/β-catenin signaling in a casein kinase 1-dependent manner. Proc. Natl. Acad. Sci. USA, *115*, E7522-E7531. https://doi.org/10.1073/pnas.1802422115.

Swanson, J. A. (1989). Phorbol esters stimulate macropinocytosis and solute flow through macrophages. J. Cell. Sci., *94*, 135–142. https://doi.org/10.1242/jcs.94.1.135.

Takai Y., Kishimoto A., Iwasa Y., Kawahara Y., Mori T., Nishizuka Y. (1979). Calcium-dependent activation of a multifunctional protein kinase by membrane phospholipids. J Biol Chem. *254*, 3692-3695.

Taelman, V. F., Dobrowolski, R., Plouhinec, J.-L., Fuentealba, L. C., Vorwald, P. P., Gumper, I., Sabatini, D. D., and De Robertis, E. M. (2010). Wnt signaling requires sequestration of glycogen synthase kinase 3 inside multivesicular endosomes. Cell, *143*, 1136–1148. https://doi.org/10.1016/j.cell.2010.11.034.

Tatarelli, C., Linnenbach, A., Mimori, K., and Croce, C. M. (2000). Characterization of the human testin gene localized in the FRA7G region at 7q31.2. Genomics, *68*, 1–12. https://doi.org/10.1006/geno.2000.6272.

Tejeda-Muñoz, N., and De Robertis, E. M. (2022a). Lysosomes are required for early dorsal signaling in the Xenopus embryo. Proc. Natl. Acad. Sci. USA, *119*, e2201008119. https://doi.org/10.1073/pnas.2201008119.

Tejeda-Muñoz, N., and De Robertis, E. M. (2022b). Wnt, GSK3, and macropinocytosis. Subcell. Biochem., *98*,169–187. https://doi.org/10.1007/978-3-030-94004-1_9.

Tejeda-Muñoz, N., Albrecht, L. V., Bui, M. H., and De Robertis, E. M. (2019). Wnt canonical pathway activates macropinocytosis and lysosomal degradation of extracellular proteins. Proc. Natl. Acad. Sci. USA, *116*, 10402–10411. https://doi.org/10.1073/pnas.1903506116.

Tejeda-Muñoz, N., Morselli, M., Moriyama, Y., Sheladiya, P., Pellegrini, M., and De Robertis, E. M. (2022). Canonical Wnt signaling induces focal adhesion and integrin beta-1 endocytosis. iScience, *25*, 104123. https://doi.org/10.1016/j.isci.2022.104123.

Tobias, E. S., Hurlstone, A. F., MacKenzie, E., McFarlane, R., and Black, D. M. (2001). The TES gene at 7q31.1 is methylated in tumours and encodes a novel growth-suppressing LIM domain protein. Oncogene, *20*, 2844–2853. https://doi.org/10.1038/sj.onc.1204433.

Vinyoles, M., Del Valle-Pérez, B., Curto, J., Viñas-Castells, R., Alba-Castellón, L., García de Herreros, A., and Duñach, M. (2014). Multivesicular GSK3 sequestration upon Wnt signaling is controlled by p120-catenin/cadherin interaction with LRP5/6. Mol. Cell, *53*, 444–457. https://doi.org/10.1016/j.molcel.2013.12.010.

Weinberg, R. A. (2007). The Biology of Cancer. (New York: Garland Science). pp. 435-461.

Wu X., Tu X., Joeng K.S., Hilton M.J., Williams D.A., Long F. (2008) Rac1 activation controls nuclear localization of beta-catenin during canonical Wnt signaling. Cell.,*133*, 340-53. doi: 10.1016/j.cell.2008.01.052.

Yoshida, S., Pacitto, R., Inoki, K., and Swanson, J. (2018). Macropinocytosis, mTORC1 and Cellular Growth Control. Cell. Mol. Life Sci., *75*, 1227–1239. doi: 10.1007/s00018-017-2710-y.

Zhitomirsky, B., and Assaraf, Y. G. (2016). Lysosomes as mediators of drug resistance in cancer. Drug Resist. Updates., *24*, 23–33. https://doi.org/10.1016/j.drup.2015.11.004.

STAR★METHODS

KEY RESOURCES TABLE

REAGENT or RESOURCE	SOURCE	IDENTIFIER
Antibodies		
GAPDH	EMD Millipore	Cat# AB2302 RRID:AB_10615768
Pak1	Abcam	Cat# ab131522, RRID:AB_11156726
FAK	Cell Signaling	Cat# 3285, RRID:AB_2269034
Rac-1	Invitrogen	Cat# PA1-091
CD63	Abcam	Cat# ab59479 RRID:AB_ 940915
TES	ATLAS	Cat# HPA018123 RRID: 1857900
ATP6V0a3	Novus	Cat# nbp1-89333 RRID:AB_11016312
β-catenin	Thermo Fisher Scientific	Cat# 71-2700; RRID:AB_ 2533982
β-catenin	Thermo Fisher Scientific	Cat# MA1-2001; RRID:AB_ 326078
Anti-mouse IgG, HRP-linked Antibody	Cell Signaling	Cat# 7076; RRID:AB_330924
Anti-rabbit IgG, HRP-linked Antibody	Cell Signaling	Cat# 7074; RRID:AB_2099233
Goat Anti-Mouse IgG H&L (Alexa Fluor® 594) preadsorbed	Abcam	Cat# ab150120; RRID:AB_2631447
Goat Anti-Rabbit IgG H&L (Alexa Fluor® 594) preadsorbed	Abcam	Cat# ab150084; RRID:AB_ 2734147
Goat Anti-Mouse IgG H&L (Alexa Fluor® 488) preadsorbed	Abcam	Cat# ab150117; RRID:AB_ 2734147
Goat Anti-Rabbit IgG H&L (Alexa Fluor® 488) preadsorbed (ab150081)	Abcam	Cat# ab150081; RRID:AB_ 2734747
Goat anti-Mouse IgG (H+L) Cross-Adsorbed Secondary Antibody, Alexa Fluor™ 488	Invitrogen	Cat# A-11001; RRID:2534069
Goat anti-Rabbit IgG (H+L) Cross-Adsorbed Secondary Antibody, Alexa Fluor™ 568	Invitrogen	Cat# A-11011; RRID:AB_143157
GSK3	Abcam	Cat# ab93926, RRID:AB_10563643
Transferrin Receptor (TfR)	ThermoFisher	Cat#13-6800
Chemicals, peptides, and recombinant proteins		
Fibronectin	ThermoFisher	Cat#33016015

Dextran Tetramethylrhodamine (TMR-Dx) 70,000	ThermoFisher	Cat# D1818
5-(N-Ethyl-N-isopropyl) amiloride (EIPA)	Sigma	Cat# A3085
Bafilomycin A1	Selleckchem	Cat# S1413
Digitonin	Sigma	Cat#300410
Phalloidin	Abcam	Cat#ab176759
Lithium chloride (LiCl)	Sigma	Cat#L4408
PF-00562271 (FAK inhibitor)	Selleckchem	Cat#S2672
Wnt3a	Peprotech	Cat#315-20
Phorbol 12-myristate 13-acetate (PMA)	TOCRIS	Cat#1201
5-(N-Ethyl-N-isopropyl) amiloride (EIPA)	Sigma	Cat# A3085
10-cm dish	ThermoFisher	Cat#174903
8-well glass-bottom chamber slides	ibidi	Cat#80827
Circular coverslips	ibidi	Cat#10815
12-well dish	ThermoFisher	Cat#150628
DMEM	ThermoFisher	Cat#11965092
L-15	ThermoFisher	Cat#11415064
Glutamine	ThermoFisher	Cat#25030081
Fetal Bovine Serum (FBS)	ThermoFisher	Cat#16000044
Bovine Serum Albumin (BSA)	ThermoFisher	Cat#9048468
Pen-Strep antibiotics	ThermoFisher	Cat#15140122
EHT 1864	Selleckchem	Catalog#S7482
Triton X-100	ThermoFisher	Cat#HFH10
Paraformaldehyde	Sigma	Cat#P6148
Fibronectin	Sigma	Cat# F4759
PBS	Gibco	Cat#10-010-023
PBS	Fisher Scientific	Cat#BP3994
Lipofectamine 3000	ThermoFisher	Cat#L3000001
Fluoroshield Mounting Medium with DAPI	Abcam	Cat# ab104139
Protease Inhibitors	Roche	Cat#04693132001
Phosphatase inhibitors	Calbiochem	Cat#524629
mMESSAGE mMACHINE™ SP6 Transcription Kit	ThermoFisher	Cat#AM1340
Critical commercial assays		
Dual-Luciferase Reporter Assay System	Promega	Cat#E1500
Experimental models: Cell lines		
HeLa (human cervical adenocarcinoma)	ATCC	RRID: CVCL_0030
SW480	ATCC	RRID:CVCL_0546
Experimental models: Organisms/strains		
Xenopus laevis	Xenopus I	
CD1 NU/NU nude mouse	Charles River Laboratories	
Recombinant DNA		
Dominant-negative (DN)-GSK3-GFP	Addgene	RRID:Addgene_29681
DN-Rab7	Addgene	#13050

pCS2-*mGFP*	Addgene	RRID:Addgene_14757
CD63-RFP	Addgene	RRID:Addgene_62964
xWnt8myc	Addgene	RRID:Addgene_16863
β-catenin Activated Reporter (BAR)	Addgene	RRID:Addgene_12456
Renilla reporter	Addgene	RRID:Addgene_62186
Software and algorithms		
ImageJ	NIH	http://imagej.nih.gov/ij/
Axiovision 4.8	Zeiss	http://Zeiss.com
Zen 2.3 imaging software	Zeiss	http://Zeiss.com
R	R Core Team	https://cran.r-project.org
Other		
IM 300 microinjection pump	Narishige International USA, Inc	N/A
Axio Observer Z1 Inverted Microscope with Apotome	Zeiss	N/A

RESOURCE AVAILABILITY

Lead contact

Further information and requests for resources and reagents should be directed to and will be fulfilled by the Lead Contact, Edward M. De Robertis.

Materials availability

No custom code, software, or algorithm central to supporting the main claims of the paper were generated in this manuscript.

Data and code availability

This paper does not report any original code.

EXPERIMENTAL MODEL AND SUBJECT DETAILS

Tissue culture and transfection

HeLa (ATCC, CRL-2648) and HEK293T cells stably expressing BAR and Renilla reporters were cultured in DMEM (Dulbecco's Modified Eagle Medium), supplemented with 10% fetal bovine serum (FBS), 1% glutamine, and penicillin/streptomycin. SW480 cells and SW480APC cells (Faux et al., 2004) were cultured in DMEM/F12 (DMEM:Nutrient Mixture F-12), supplemented with 5% FBS, 1% glutamine, and penicillin/streptomycin. The cells were seeded at a cell density of 20 to 30%, and experiments were performed when cells reached between 70 to 80% confluency. Cells were cultured for 6 to 8 hours in a medium containing 2% FBS before all treatments.

Xenopus embryo microinjection

All animal experiments were as approved by the UCLA Animal Research Committee. *Xenopus laevis* embryos were fertilized *in vitro* using excised testis, and staged as described (Colozza and De Robertis 2014; Tejeda-Muñoz and De Robertis, 2022a). *In vitro* synthesized mRNAs were introduced into embryos by microinjection using an IM 300 Microinjector (Narishige International USA, Inc) of 4 nl into the marginal zone of a ventral blastomere at the 4-cell stage. pCS2-DN-GSK3β, β-catenin, and DN-Rab7 were linearized with NotI and transcribed with SP6 RNA

polymerase using the Ambion mMessage mMachine kit. Embryos were injected in 1x MMR and cultured in 0.1x MMR.

Bisected embryo TMR-dextran staining

Xenopus embryos at late blastula/early gastrula stage were injected into the blastula cavity with 40 nl TMR-dextran 70 kDa. Embryos were incubated in 0.1 × MMR solution until stage 11. Embryos were collected and fixed with 4% PFA (paraformaldehyde, Thermo Scientific, 28908), diluted in 1× PBS (Fisher Scientific, BP399-4). After 24 hours of fixation, embryos were cut along the D–V axis with a surgical blade and refixed with 4% PFA for 15 minutes. Embryos were then washed with PBS three times, blocked with 5% bovine serum albumin (BSA) in PBS to reduce background for 24 hours, then washed three times with PBS. Embryos were plated in agar Petri dishes with PBS for microscopic examination as soon as possible to avoid bleaching of fluorescence. Samples were imaged using an Axio Zoom.V16 Stereo Zoom Zeiss microscope with apotome function, and stacked images were reconstructed using the Zen 2.3 Pro Zeiss software.

Human colon cancer tissue array and immunochemistry

Three sets of colon cancer tissue arrays containing 90 cases of adenocarcinoma and 90 adjacent normal colon tissue (180 tissue cores total) were obtained from TissueArray.com. The company stated that each specimen collected from any clinic was consented to by both the hospital and the individual, and that discrete legal consent forms were obtained and the rights to hold research uses for any purpose or further commercialized uses were waived. Double stained immunohistochemistry was performed on paraffin-embedded tissue samples which were

deparaffinized in xylene and rehydrated using graded alcohols. For antigen retrieval, slides were incubated at 95°C for 40 minutes in citrate buffer (10 mM, 0.05% Tween 20, pH 6.0). Tissue sections were than fixed with 4% paraformaldehyde (Sigma #P6148) for 15 minutes, treated with 0.2% Triton X-100 in phosphate-buffered saline (PBS; Gibco) for 10 minutes, and blocked with 5% BSA in PBS overnight. Primary and secondary antibodies were added overnight at 4°C. The samples were washed three times with PBS after each treatment, and coverslips were mounted with Fluoroshield Mounting Medium with DAPI (ab104139). Immunofluorescence was analyzed and photographed using a Zeiss Imager Z.1 microscope with Apotome.

Xenograft tumor model

For the CD1 NU/NU nude mouse model, SW480 cells were collected by trypsinization. Then, 7.5 x 10^5 cells per injection site were resuspended in high-concentration Matrigel (BD Biosciences, Franklin Lakes, NY), diluted in PBS to 50% final concentration, and subcutaneously injected into the flanks of an 8-week-old mouse. After day 7, when the tumor was established, the tumor was measured 3 times a week until completion. After three weeks, tissue was obtained from animals euthanized by CO2 inhalation. Tumor and normal colon were fixed, paraffin-embedded, and 5 μm histological sections were mounted on slides. Mouse experiments were approved by the UCLA Animal Research Committee.

Antibodies and reagents

Total β-catenin antibody (1:1,000) was purchased from Invitrogen (712700), glyceraldehyde-3-phosphate dehydrogenase antibody (1:1,000) and FAK antibody (1:1,000, 3285) were obtained

from Cell Signaling Technologies, anti-ATP6V0a3 antibody (1:500) was obtained from Novus (nbp1-89333, 1:1,000). CD63 antibody was obtained from Abcam. Antibodies against Pak1 (ab131522), Ras (ab52939), GSK3 (ab93926, 1:4000), and secondary antibodies for immunostaining for cells (ab150120, ab150084, ab150117, ab150081) (1:300) were obtained from Abcam. Antibody against the focal adhesion protein Tes (HPA018123, 1:100) was obtained from Atlas antibodies. Secondary antibodies for immunostaining arrays (A-11001, A-11011 were obtained from Invitrogen). HRP-linked secondary antibodies (7076, 7074 at 1:5000 (Cell Signaling) were used for Western blots and analyzed with an iBright Imaging system. EIPA (A3085), and LiCl (L4408), were obtained from Sigma. Baf (S1413) and PF-00562271 (FAK inhibitor, S2672) were purchased from Selleckchem. TMR-dextran 70 kDa was obtained from ThermoFisher (D1818). PMA (1201) was purchased from TOCRIS.

METHOD DETAILS

Immunostainings

HeLa, HEK293T, SW480, and SW480APC cells were plated on glass coverslips and transferred to 2% FBS 6 to 12 hours before overnight experimental treatments. Coverslips were acid-washed and treated with Fibronectin (10 μg/ml for 30 min at 37ºC, Sigma F4759) to facilitate cell spreading and adhesion. Cells were fixed with 4% paraformaldehyde (Sigma #P6148) for 15 minutes, permeabilized with 0.2% Triton X-100 in phosphate-buffered saline (PBS; Gibco) for 10 minutes, and blocked with 5% BSA in PBS for 1 hour. Primary antibodies were added overnight at 4°C. Cells were washed three times with PBS, and secondary antibodies were applied for one hour at room temperature. After three additional washes with PBS, the coverslips were mounted

with Fluoroshield Mounting Medium with DAPI (ab104139). Immunofluorescence was analyzed and photographed using a Zeiss Imager Z.1 microscope with Apotome.

Western blots

Cell lysates were prepared using RIPA buffer (0.1% NP40, 20 mM Tris/HCl pH 7.5), 10% Glycerol, together with protease (Roche #04693132001) and phosphatase inhibitors (Calbiochem #524629), and processed as described (Tejeda-Muñoz et al., 2019).

Luciferase assay

Experiments were performed with stably transfected HEK293T cells stably expressing BAR and Renilla reporters (Albrecht et al., 2020), treated with LiCl and with or without Bafilomycin for 8 hours, and Luciferase activity measured with the Dual-Luciferase Reporter Assay System (Promega) according to the manufacturer's instructions, using the Glomax Luminometer (Promega). Luciferase values of each sample were normalized for Renilla activity.

3D spheroid cell culture

SW480 cells were cultured in a petri dish using DMEM:F-12 medium with 5%FBS. The top cover was removed from 60 mm tissue culture dishes and 3 mL of PBS placed in the bottom of the dish to act as a hydration chamber. Cells were counted and 500 cells were added as 25 µL drops deposited onto the Petri dish cover, and immediately inverted over the humid chamber. At least 6 drops per condition were plated, keeping enough distance between each other. The inverted drop cultures were incubated at 37°C in 5% CO_2/95% humidity. The drops were monitored daily; after

4 days, aggregates had been formed and EHT treatment was added to the spheroids. After 4 days, spheroids were incubated with TMR-dextran 70kDa (1 mg/ml) for 1 hour, and each spheroid was photographed with an Axio Zoom.V16 Stereo Zoom Zeiss microscope with apotome function.

Bafilomycin treatments in *Xenopus* embryos

We determined that optimal ventralization with loss of head structures of *Xenopus* embryos was obtained after incubation with Baf (5 μM) for 7 minutes at the 32-cell stage in 0.1 x MMR solution. After incubation, embryos were washed two times with 0.1 x MMR solution and cultured overnight until early tailbud tadpole stage. Embryos were microinjected once ventrally at the four-cell stage with any of the following reagents: LiCl (300 mM), PMA (500 nM), EIPA (1 mM), EHT (1 mM), or mRNAs like DN-GSK3-β (150 pg), DN-Rab-7 (500 pg) and Wnt8 (2 pg), either alone or co-injected with the other reagents. After this, embryos were incubated in 0.1 x MMR solution until the 32-cell stage. Embryos that were previously injected with any of the previous treatments were then transferred to 0.1 x MMR solution with or without Baf (5 μM) and incubated for 7 minutes. Embryos were then washed twice with 0.1 x MMR solution and cultured until tadpole stage.

LiCl and Bafilomycin sequential treatments

Whole embryos at the 32-cell stage were incubated with LiCl (300 mM) alone for 7 min. After this treatment, the embryos were washed 2 times with 0.1 x MMR solution and cultured until the tadpole stage, or incubated again for 7 min in 0.1 MMR solution containing 5 μM Baf, and washed

as described before. In the converse experiment, embryos were first treated with Baf and then with LiCl. All treatments were done at the 32-cell stage, which plays a key role in the early Wnt signal (Kao et al., 1986; Tejeda-Muñoz and De Robertis, 2022).

qRT-PCR

Quantitative RT-PCR experiments using *Xenopus* embryos were performed as previously described (Colozza and De Robertis, 2014). Primer sequences for qRT-PCR were as follows:

Gene	Forward	Reverse	Use
ODC	CAGCTAGCTGTGGTGTGG	CAACATGGAAACTCACACC	qRT-PCR
Siamois	AAGATAACTGGCATTCCTGAGC	GGTAGGGCTGTGTATTTGAAGG	qRT-PCR
Xnr3	CGAGTGCAAGAAGGTGGACA	ATCTTCATGGGGACACAGGA	qRT-PCR
Sizzled	GTCTTCCTGCTCCTCTGC	AACAGGGAGCACAGGAAG	qRT-PCR
Vent1	GGCACCTGAACGGAAGAA	GATTTTGGAACCAGGTTTTGAC	qRT-PCR

QUANTIFICATION AND STATISTICAL ANALYSIS

Data were expressed as means and SEMs. Statistical analysis of the data was performed using the student t-test; a P-value of <0.01** was considered statistically significant for differences between means. Fluorescence was quantified in control versus treated cells using ImageJ software analyses with n>30 cells or n>30 images from arrays from humans or mouse sample per condition. Fluorescence intensity was normalized in images compared in each condition and results from three or more independent experiments were presented as the mean ± SEM.

Figure Legends

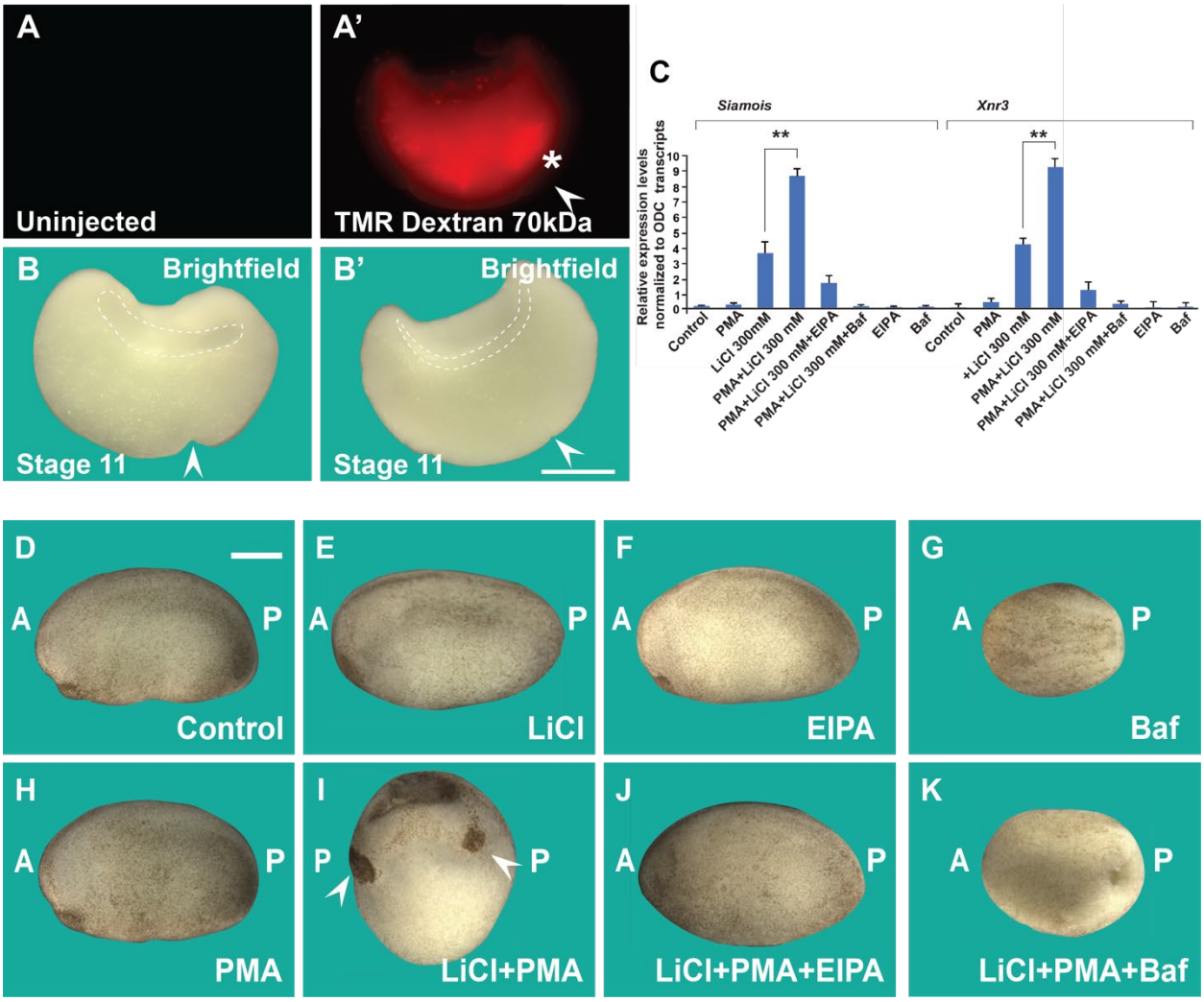

Figure 1. The Phorbol Ester PMA Synergizes with GSK3 Inhibition and this Cooperation Requires Macropinocytosis and Lysosome Acidification

(A-A') Albino mbryos injected into the gastrula cavity (40 nl at 1 mM) with the macropinocytosis marker TMR-dextran 70kDa were fixed and bisected at gastrula stage 11. Note that dextran macropinocytosis is stronger in the dorsal part of the embryo (asterisk; dorsal blastopore indicated by arrowhead).
(C) PMA increases the effects of LiCl in Wnt signaling in early embryos. qRT-PCR analysis at blastula stage 9.5 of the Wnt target genes *Siamois* and *Xnr3* normalized for Ornithine decarboxylase (ODC) transcripts. Embryos received a single injection of 4 nl of LiCl (300 mM with or without PMA (500 nM).
(D) Uninjected control embryo at stage 24.

(E) LiCl (4nl 300 mM, 1 x ventral) dorsalized the embryo only slightly.
(F) EIPA (1 mM, 1x ventral) alone did not produce a distinctive phenotype at this concentration.
(G) The vacuolar ATPase (V-ATPase) inhibitor Bafilomycin A1 (Baf) (incubation with 5 μM for 7 minutes at 32 cells) ventralized embryos.
(H) A single injection of PMA (500 nM) did not show any phenotypic effect.
(I) PMA and LiCl strongly synergized, resulting in embryos with radial heads.
(J) Coinjection of the EIPA macropinocytosis inhibitor blocked dorsalization caused by LiCl plus PMA.
(K) Incubation with Baf lysosomal acidification inhibitor blocked dorsalization caused by LiCl plus PMA.
Number of embryos or hemisections analyzed were as follows: A = 150, 100%; A' = 160, 97% with fluorescence; five independent experiments; D = 70, 100%; E = 80; 98%; F = 75, 94%; G = 82, 92%; H = 76, 100%; I = 112, 98% J = 75, 93%; K = 85, 98%. Scale bars, 500 μm ; Error bars denote SEM ($n \geq 3$) (**$P < 0.01$).
Also see Figure S1.

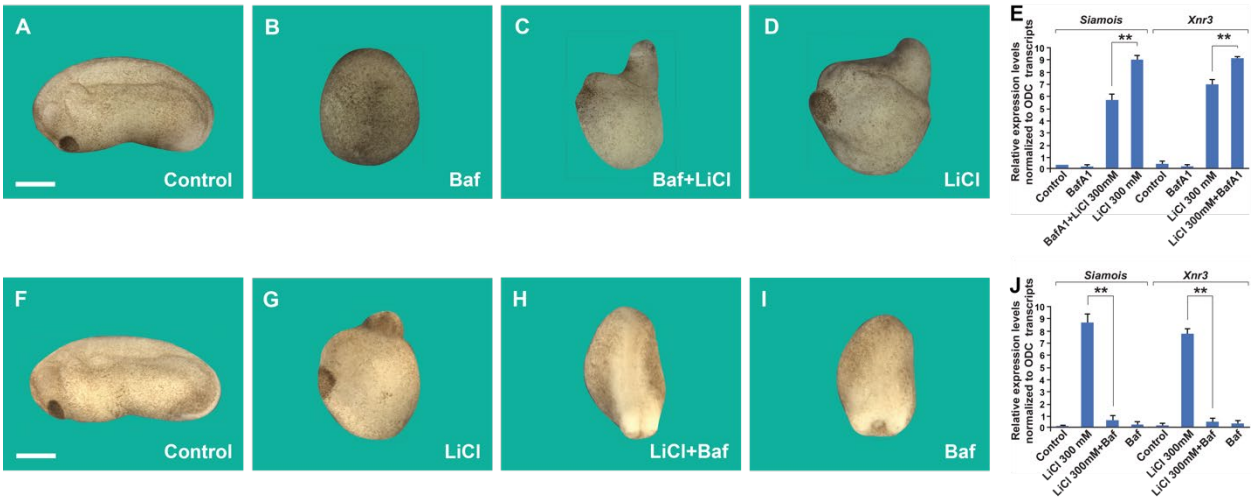

Figure 2. Order-of-addition Experiment Showing that Lysosomal Acidification at 32-cell Stage is Required for Early Wnt/β-catenin Activation

(A) Untreated embryo.
(B) Baf treatment (5 μM for 7 minutes) inhibited endogenous axis formation resulting in ventralized embryos lacking heads at early tailbud.
(C) Embryos treated with Baf, washed, and then immersed in 300 mM LiCl an additional 7 minutes formed heads, resulting in dorsalized embryos with enlarged heads and short trunks. Note that all treatments were done at 32-cell stage, which is critical for the early Wnt signal.
(D) LiCl treatment alone dorsalized embryos.
(E) Quantitative RT-PCR (qPCR) for Wnt target genes *Siamois* and *Xnr3* at blastula, confirming that the phenotypic effects are due to early activation of the Wnt pathway.
(F) Untreated embryo.
(G) Embryos incubated with LiCl at 32-cell were dorsalized.
(H) Embryos first treated with LiCl and then subsequently with Baf resulted in ventralized embryos lacking heads.
(I) Baf treatment caused ventralization and small heads.
(J) Quantitative RT-PCR for Wnt target genes *Siamois* and *Xnr3* showing that inhibiting V-ATPAse at the 32-cell stage blocks the effect of earlier LiCl treatment.
The numbers of embryos analyzed were as follows: A = 115, 100% B = 124, 98% with phenotype; C = 132, 97% ; D 99% ; F = 132, 100% ; G = 135, 99% ; H = 126, 97% ; I = 129, 98% (Scale bars, 500 μm.). Error bars denote SEM ($n \geq 3$) (**$P < 0.01$).

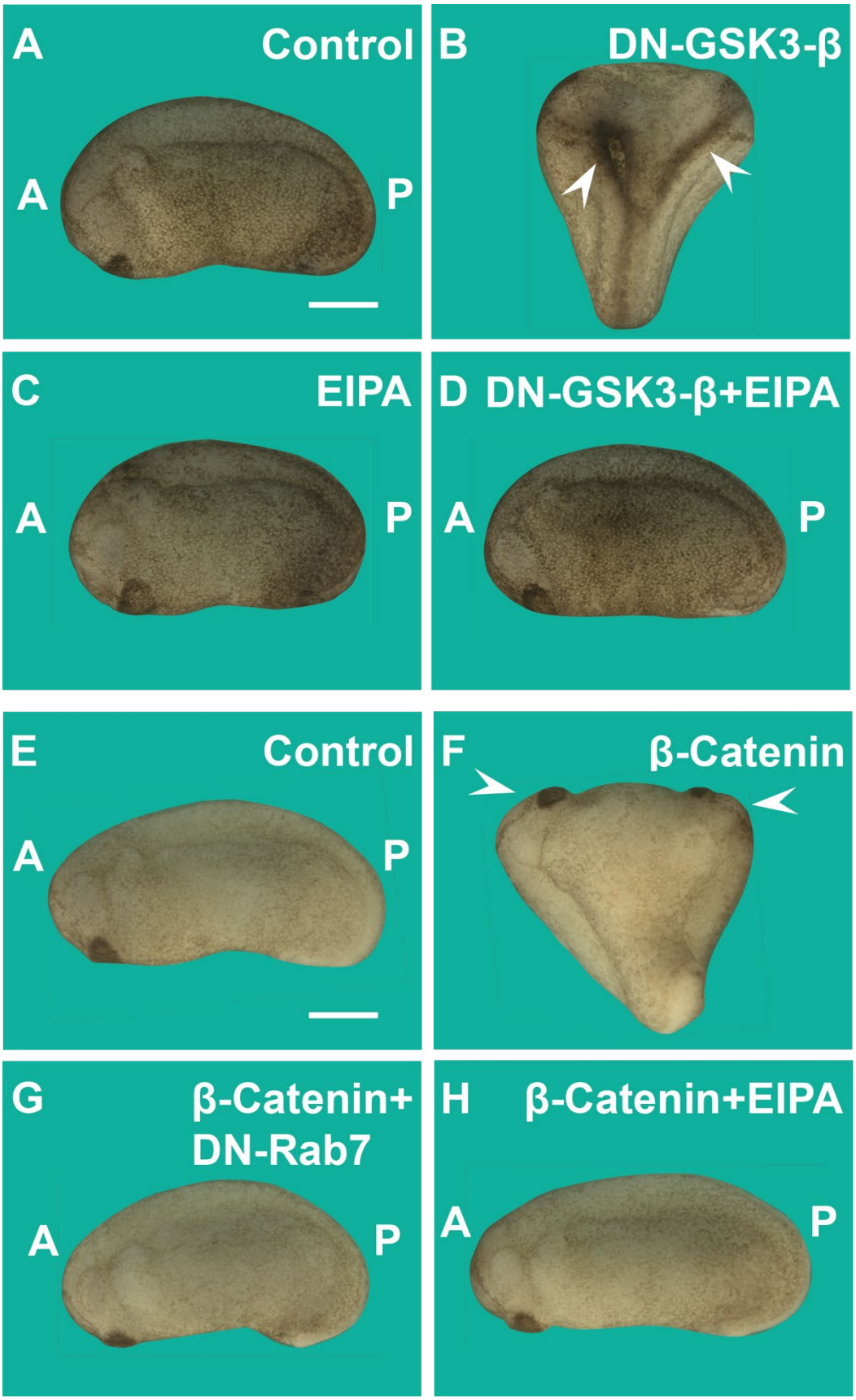
A
Control
A
P
B
DN-GSK3-β
C
EIPA
A
P
D
DN-GSK3-β+EIPA
A
P
E
Control
A
P
F
β-Catenin
G
β-Catenin+
DN-Rab7
A
P
H
β-Catenin+EIPA
A
P

Figure 3. Induction of Secondary Axes by the GSK3/β-catenin Pathway Requires Membrane Trafficking

(A) Control embryo at early tailbud.
(B) Embryo injected with DN-GSK3 (dominant-negative GSK3-β, 150 pg 1 x ventral) mRNA, showing double axes (arrowheads).
(C) Injection of EIPA 1 x ventral alone showed no phenotypic effect (4 nl,1 mM).
(D) Coinjection of DN-GSK3 and EIPA blocked double axis formation.
(E) Uninjected control embryo.
(F) Activation of Wnt signaling via injection of β-catenin mRNA (80 pg) induced complete twinned axes (arrowheads).
(G) Embryo coinjected with β-catenin mRNA and DN-Rab7 (500 pg) showing that membrane trafficking is required for secondary axis formation.
(H) Coinjection of β-catenin mRNA and the macropinocytosis inhibitor EIPA blocks axial duplication.
The numbers of embryos analyzed were as follows: A = 62, 100%; B = 75, 94% with double axes; C = 76, 100%; D = 70; 98%; E = 70, 100%; F = 73, 98%; G= 69, 75%; H = 82, 97%; four independent experiments; (Scale bars, 500 μm.). Error bars denote SEM ($n \geq 3$) (**$P < 0.01$).

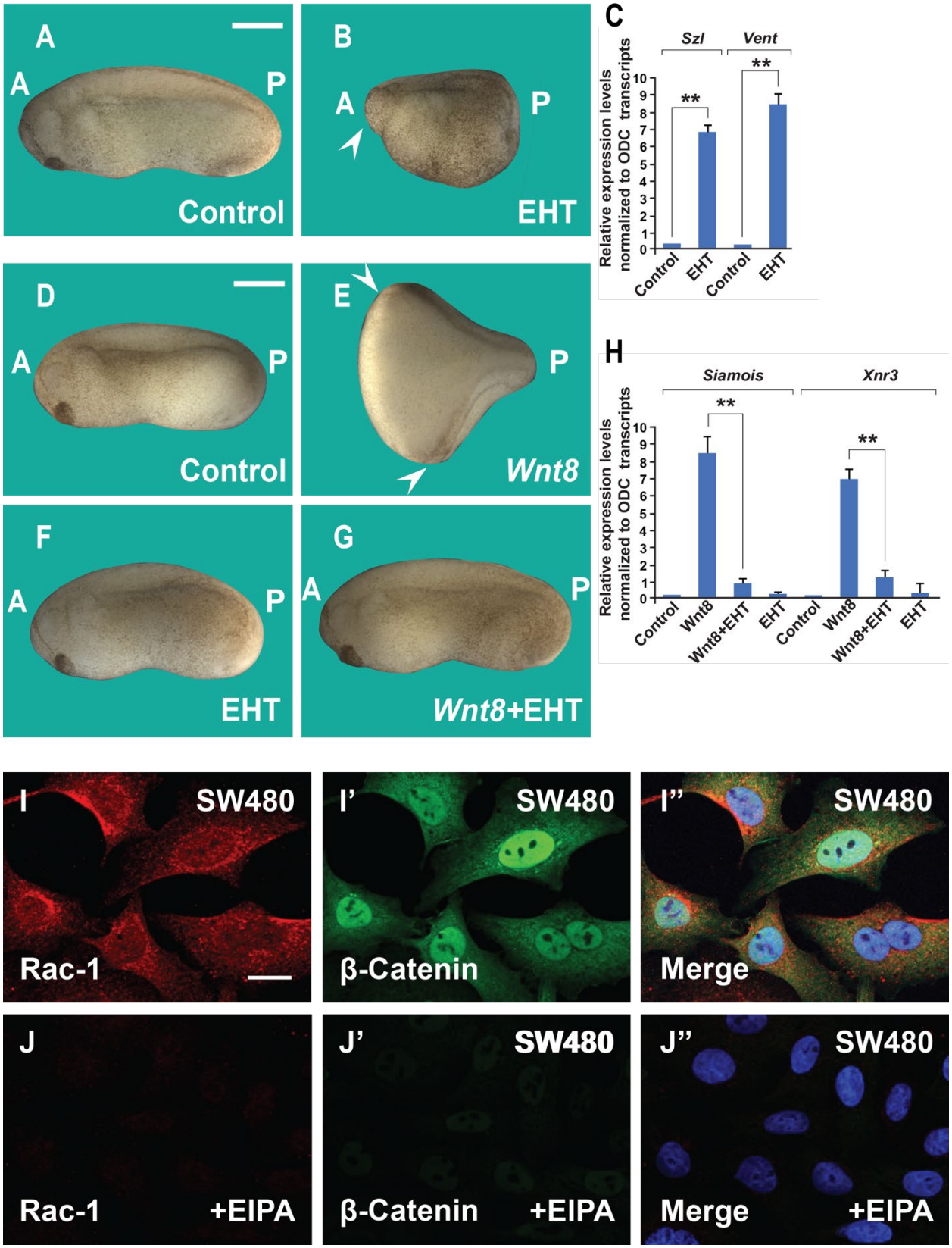
A
A
P
Control
B
A
P
EHT
C
Szl
Vent
Relative expression levels normalized to ODC transcripts
**
**
Control
EHT
Control
EHT
D
A
P
Control
E
P
Wnt8
F
A
P
EHT
G
A
P
Wnt8+EHT
H
Siamois
Xnr3
Relative expression levels normalized to ODC transcripts
**
**
Control
Wnt8
Wnt8+EHT
EHT
Control
Wnt8
Wnt8+EHT
EHT
I
SW480
Rac-1
I'
SW480
β-Catenin
I''
SW480
Merge
J
Rac-1
+EIPA
J'
SW480
β-Catenin
+EIPA
J''
SW480
Merge
+EIPA

Figure 4. Rac1 Inhibitor EHT1864 Blocks Wnt Signaling in *Xenopus* Embryos, and Macropinocytosis Is Required for Nuclear β-catenin Accumulation in CRC Cells

(A) Uninjected control embryo.
(B) Incubation of the *Xenopus* embryos with the Rac1 inhibitor EHT at 32-cell stage (7 min, 10 mM) resulted in a ventralized phenotype with a small head in the anterior (A, arrowhead) and expanded ventral structures in the posterior (P). Rac1 activity is required for macropinocytosis, see Figure S2).
(C) qRT-PCR of gastrula stage embryos showing increased ventral markers Szl and Vent1 after Rac1 inhibition.
(D) Control embryo.
(E) Injection of Wnt8 mRNA (2 pg) induces complete duplicated axes (arrows).
(F) Injected embryos with EHT (1 mM, 4 nl 1 x ventral) alone showed no phenotypic effect at this concentration.
(G) EHT coinjected with Wnt8 mRNA blocked double axis formation.
(H) qRT-PCR of Wnt target genes *Siamois* and Xnr3 at blastula confirming that Rac1 is required for early Wnt signaling.
(I-I') The colorectal cancer cell line SW480, in which the Wnt signaling pathway is activated by APC mutation, was positive for Rac1 and nuclear β-catenin immunostaining.
(I'') Merged panel including the DNA stain DAPI.
(J-J'') SW480 cells treated with the EIPA inhibitor (40 μM) had strongly decreased Rac1 and nuclear β-catenin levels, indicating a requirement for macropinocytosis.
The numbers of embryos analyzed were as follows: A = 52, 100%; B = 47, 95% with ventralized small head phenotype; D = 58, 100%; E = 67; 97%; F = 64, 96%; G = 62, 97%; four independent experiments. Scale bars for embryos 500 μm; scale bars for immunofluorescence, 10 μm. Experiments represent biological replicates. Error bars denote SEM ($n \geq 3$) (**$P < 0.01$). Also see Figure S2.

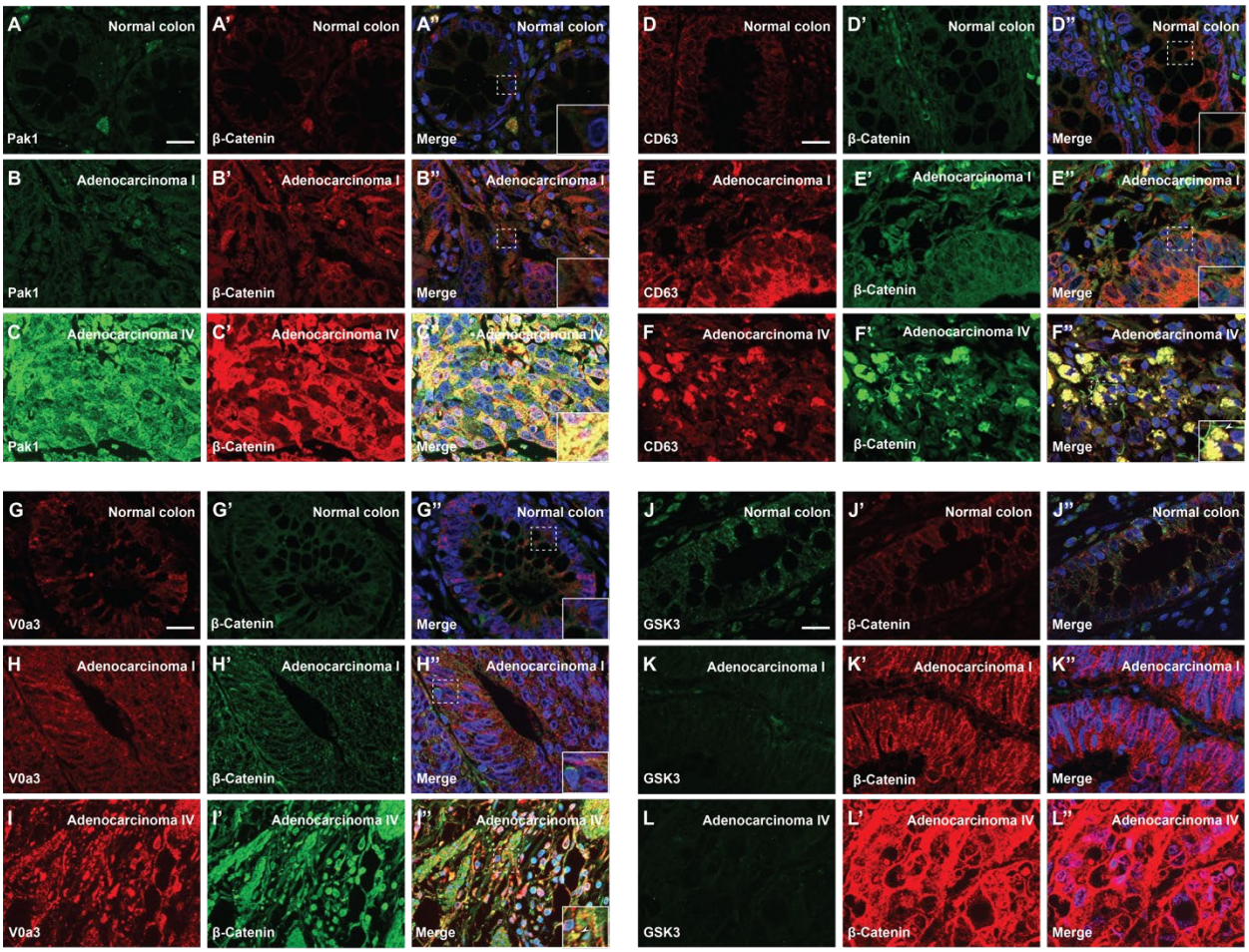

Figure 5. Degree of Human CRC Malignancy is Associated with Increased Macropinocytosis/MVB/lysosome markers and decreased GSK3 levels

(A-A') Normal human colon paraffin section stained with the macropinocytosis marker Pak1 and β-catenin, respectively.
(A'') Merged image with DAPI, a few cells colocalize both markers.
(B-B'') Pak1 and β-catenin levels are moderately increased at an early stage I CRC adenocarcinoma.
(C'-C'') Strong colocalization between Pak1 and β-catenin was observed in advanced stage IV CRC (inset).
(D-D'') Normal human colon section stained with the MVB marker CD63 and β-catenin; colocalization was not observed.
(E-E'') CD63 and β-catenin were stabilized in adenocarcinoma I, and moderate colocalization was found between CD63 and β-catenin.
(F-F') CD63 and β-catenin were strongly stabilized and colocalized in adenocarcinoma stage IV CRC.
(F'') Merge; note the striking colocalization between the MVB marker CD63 and β-Catenin in advanced stages of cancer (inset).

(G-G'') Normal colon stained for V0a3 (a subunit of V-ATPase that marks lysosomes) and β-catenin.
(H-H'') Stage I adenocarcinoma with moderately increased levels of lysosomes and β-catenin.
(I-I'') Strong co-localization of lysosomes and β-catenin in stage IV CRC (see inset).
(J-J'') Human colon array stained with the GSK3 and β-catenin.
(K-K'') GSK3 decreases, and β-catenin increases, at early stages of carcinogenesis,
(L-L'') GSK3 levels are very low in advanced CRC compared to normal human colon, while β-catenin levels are very high.
Scale bars, 10 μm. Also see Figure S3 for quantifications and mouse xenografts of CRC cells.

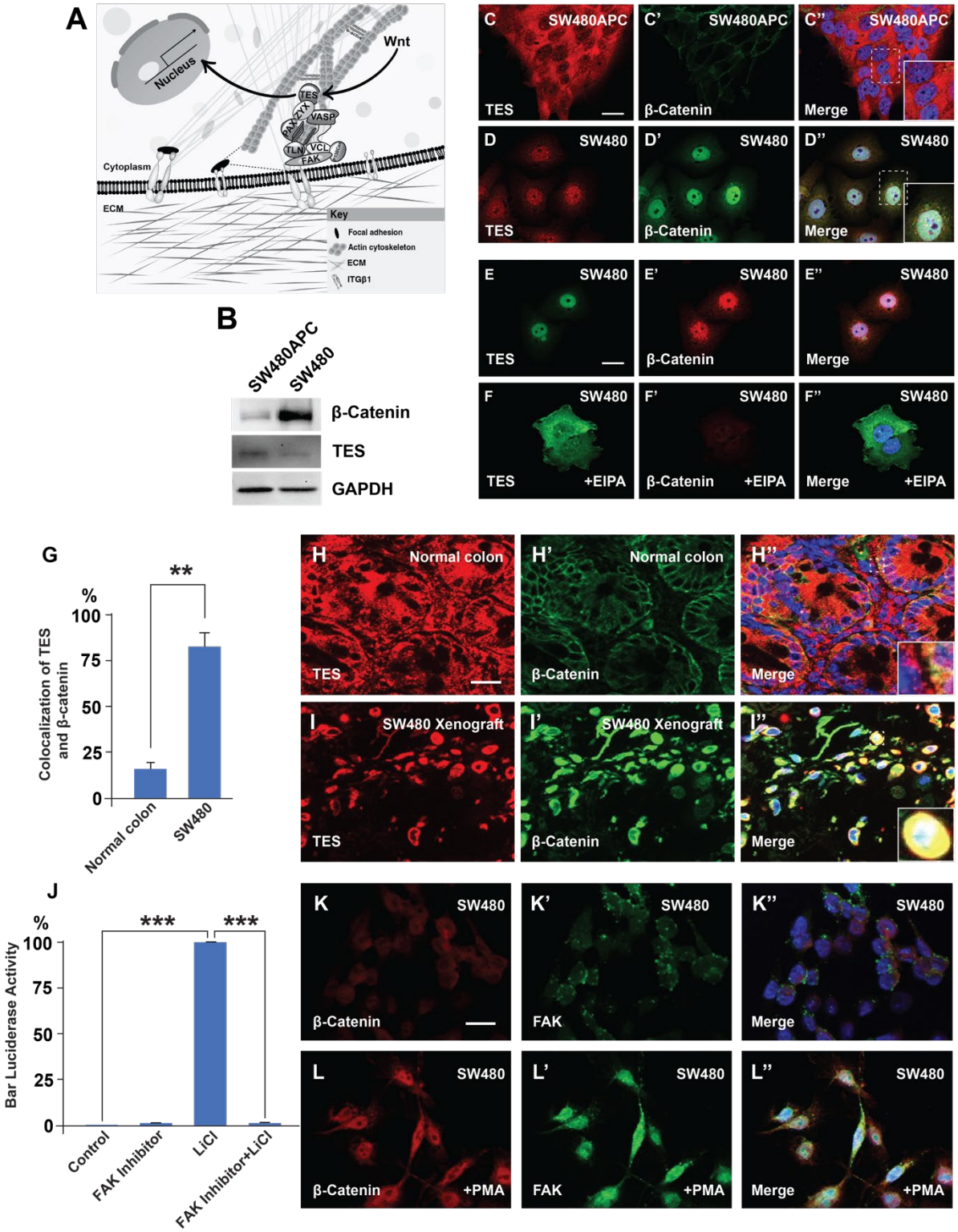
A
Nucleus
Wnt
TES
VASP
PAXX
TLN
VCL
FAK
Cytoplasm
ECM
Key
Focal adhesion
Actin cytoskeleton
ECM
ITGβ1
B
SW480APC
SW480
β-Catenin
TES
GAPDH
C SW480APC TES
C' SW480APC β-Catenin
C'' SW480APC Merge
D SW480 TES
D' SW480 β-Catenin
D'' SW480 Merge
E SW480 TES
E' SW480 β-Catenin
E'' SW480 Merge
F SW480 TES +EIPA
F' SW480 β-Catenin +EIPA
F'' SW480 Merge +EIPA
G
**
%
100
75
50
25
0
Colocalization of TES and β-catenin
Normal colon
SW480
H Normal colon TES
H' Normal colon β-Catenin
H'' Merge
I SW480 Xenograft TES
I' SW480 Xenograft β-Catenin
I'' Merge
J
***
***
%
100
75
50
25
0
Bar Luciderase Activity
Control
FAK Inhibitor
LiCl
FAK Inhibitor+LiCl
K SW480 β-Catenin
K' SW480 FAK
K'' SW480 Merge
L SW480 β-Catenin +PMA
L' SW480 FAK +PMA
L'' SW480 Merge +PMA

Figure 6. A Focal Adhesion Protein Changes Its Nucleocytoplasmic Distribution after Wnt Signaling Activation, and FAK is Stabilized by PMA

(A) Diagram showing how focal adhesions connect the actin cytoskeleton to the extracellular matrix via integrins; Wnt signaling changes the distribution of the focal adhesion protein Tes from focal adhesion sites to the nucleus.
(B) Western blot of SW480 cells with and without stable expression of APC; note the reduction in Tes expression and increase in β-catenin levels in SW480 cells lacking full-length APC. GADPH was used as loading control.
(C-C') Colon cancer cell line SW480 stably restored with full-length APC stained with Tes and β-catenin antibodies; note that in SW480APC cells TES is absent from the nucleus (inset).
(D-D'') In SW480 CRC cells both Tes and β-catenin are located the nucleus.
(E-E'') Colon cancer cell line SW480 stained with Tes (in green) and β-catenin (in red) antibodies as a control.
(F-F'') Inhibiting macropinocytosis with EIPA (40 μM) treatment restored the cytoplasmic localization of the focal adhesion protein Tes in SW480 cells and strongly inhibited β-catenin levels.
(G) Quantification of colocalization between Tes and β-catenin in normal mouse colon and SW480 xenografts.
(H-H') Immunohistochemistry of the CD1 NU/NU normal mouse colon showing Tes and β-catenin distribution.
(H'') Merge showing modest co-localization (inset).
(I-I'') Immunohistochemistry images of the CD1 NU/NU mouse xenograft model showing nuclear TES, which is strongly colocalized with β-catenin levels in cancer cells (inset).
(J) Reporter assay in HEK293T cells stably expressing BAR and Renilla, showing strong inhibition of the β-catenin transcriptional activity induced by LiCl (40 mM) by FAK inhibitor PF-00562271 (20 μM) after overnight treatment. See also Figure S4A-S4B''.
(K-K'') SW480 cells immunostained with FAK and β-catenin antibodies.
(L-L'') The tumor promoter PMA (750 nM, overnight treatment) increased levels of both β-catenin and FAK in SW480 cells (in which the Wnt pathway is constitutively activated by APC mutation). This increase in FAK levels requires membrane macropinocytosis and lysosome activity (see Figure S4C-S4H'').
Error bars denote SEM ($n \geq 3$) (**$P < 0.01$) (Scale bars, 10 μm).
Also see Figure S4.

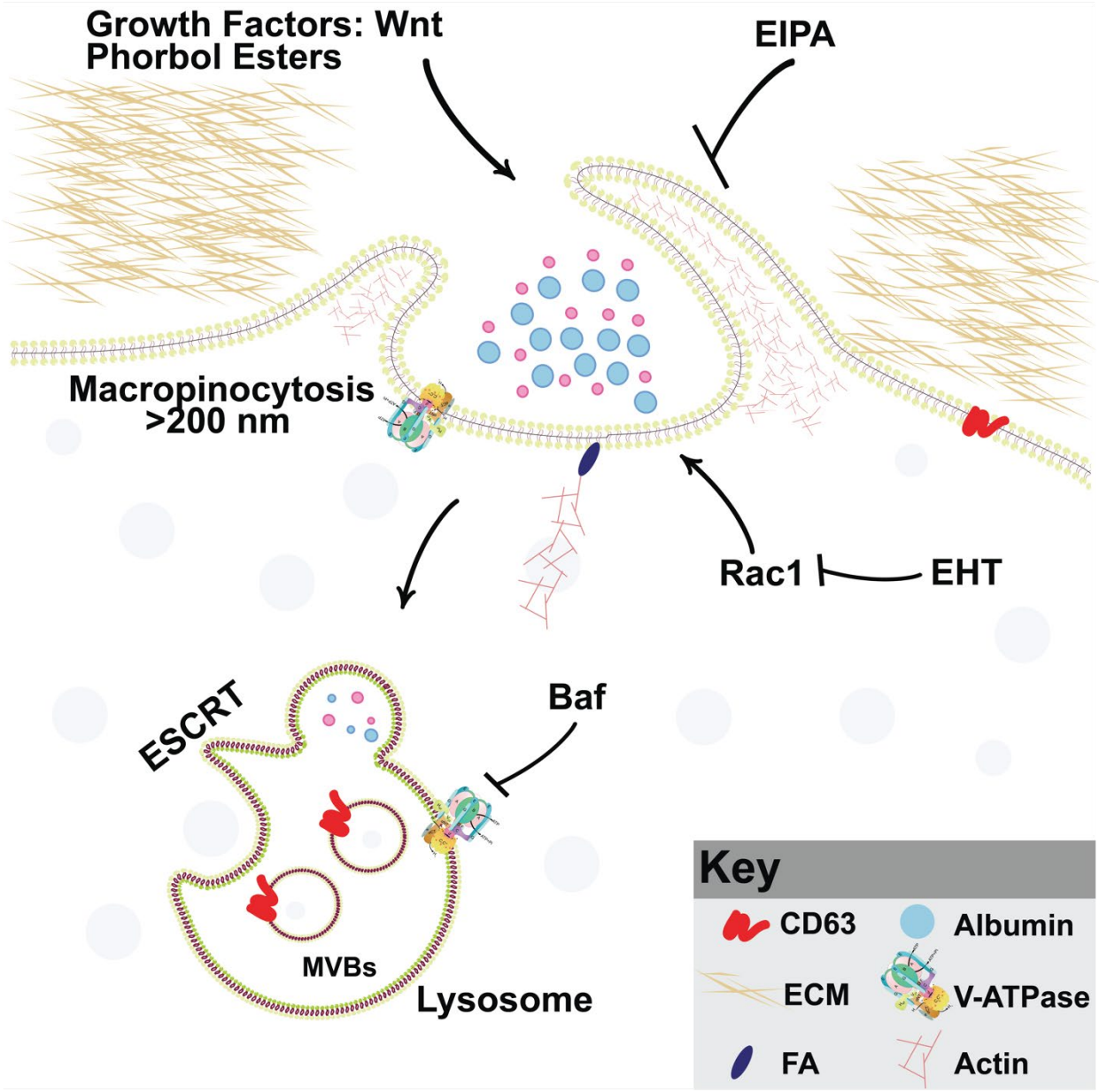

Figure 7. Model of PMA Synergy with Wnt Signaling through Macropinocytosis and Membrane Trafficking

Wnt and PMA are activators of macropinocytosis, which is a cell drinking process driven by an actin meshwork that requires the small GTPase Rac1. Membrane trafficking into MVBs/lysosomes (marked by CD63) requires acidification by V-ATPase, which is inhibited by Bafilomycin A (Baf). Phorbol esters such as PMA stimulate macropinocytosis and synergize with Wnt signaling. Inhibiting macropinocytosis with the membrane trafficking inhibitors EIPA, Baf, or the Rac1 inhibitor EHT1864 block Wnt signaling and its cooperation with the tumor promoter PMA.

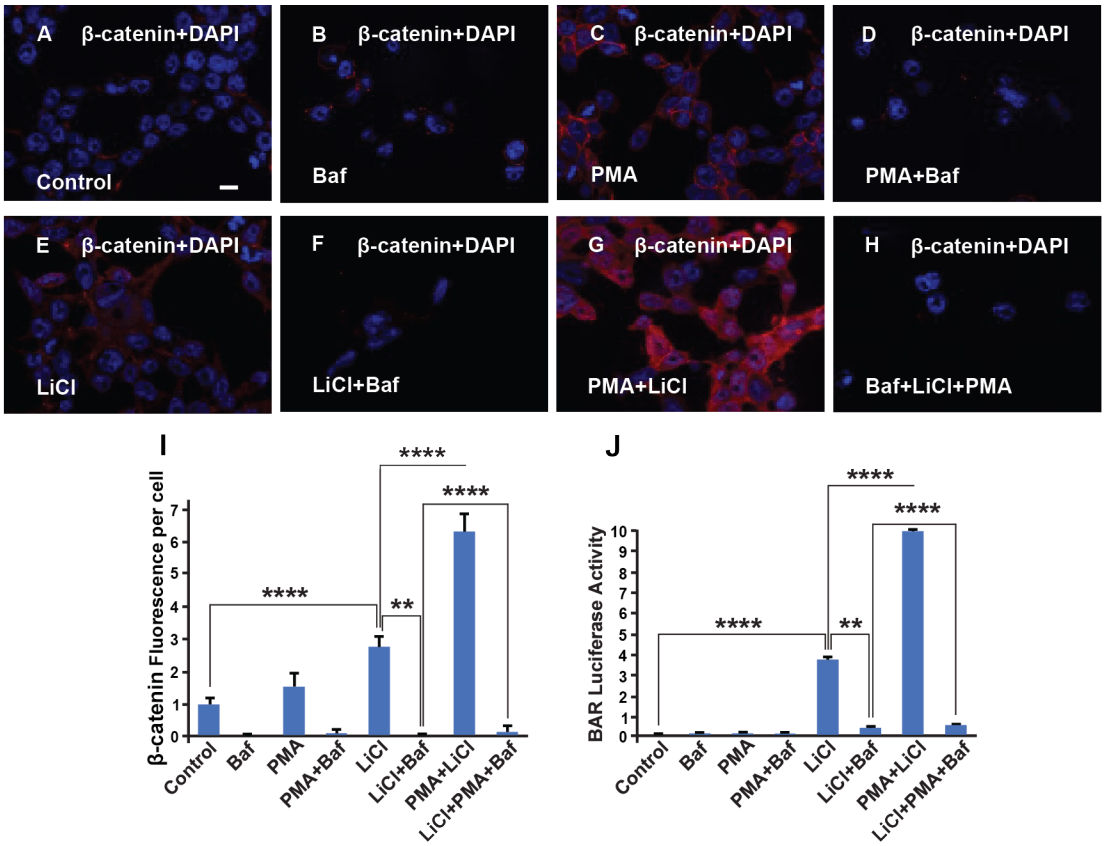

Supplementary Figure S1. In Cultured Cells, the Phorbol Ester PMA Cooperates with GSK3 Inhibition in β-catenin Signaling, and this Requires Lysosomal Acidification; Related to Figure 1

(A) HEK293BR (BAR/Renilla) cells stained with total β-catenin antibody.
(B) HEK293BR cells treated with Baf (20 μM) overnight show no changes in β-catenin levels.
(C) Treatment with PMA (1.5 μM) slightly increased β-catenin levels.
(D) HEK293BR cells treated with PMA and Baf had low β-catenin levels.
(E) Cells treated with LiCl (40 mM) showed an increase in β-catenin.
(F) Baf treatment blocked the increase in β-catenin caused by LiCl.
(G) PMA cooperated with LiCl in the induction of β-catenin levels.
(H) Baf treatment blocked the cooperative effect of LiCl and PMA, indicating a requirement for lysosome acidification.
(I) Quantification of β-catenin fluorescence per cell with the different treatments indicated above.
(J) Luciferase assay in HEK293BR cells showing cooperation between PMA and LiCl, and its inhibition by Baf.
All experiments with cultured cells were biological triplicates. Error bars denote SEM ($n \geq 3$) (**$P < 0.01$). (Scale bar, 10 μm.).

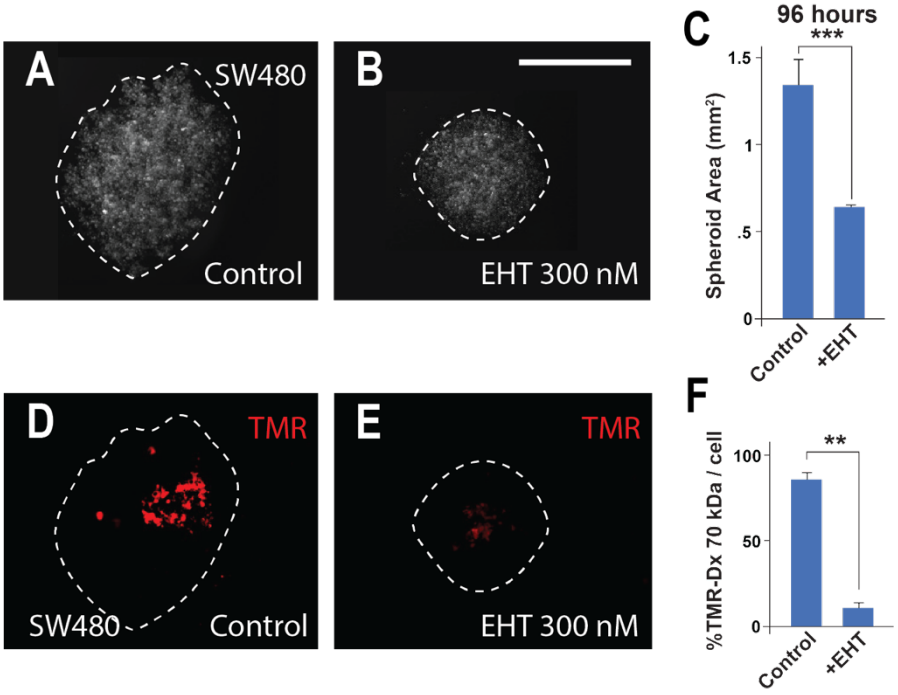

Supplementary Figure S2. Macropinocytosis is Inhibited in SW480 CRC Spheroids by Treatment with the Rac1 Inhibitor EHT; Related to Figure 4

(A) Control SW480 spheroids at 96 hours of inverted drop culture.
(B) Treatment with 300 nM Rac1 inhibitor (EHT1864) reduced the diameter of SW480 spheroids at 96 hours.
(C) Quantification of spheroid area after EHT treatment.
(D) The same spheroids incubated with the macropinocytosis marker TMR-dextran 70kDa for 1 hour.
(E) EHT treatment strongly inhibited macropinocytosis.
(F) Quantification of macropinocytosis inhibition.
Six spheroids were plated per condition, in triplicate. Error bars denote SEM ($n \geq 3$) (**$P < 0.01$). (Scale bars, 500 µm.).

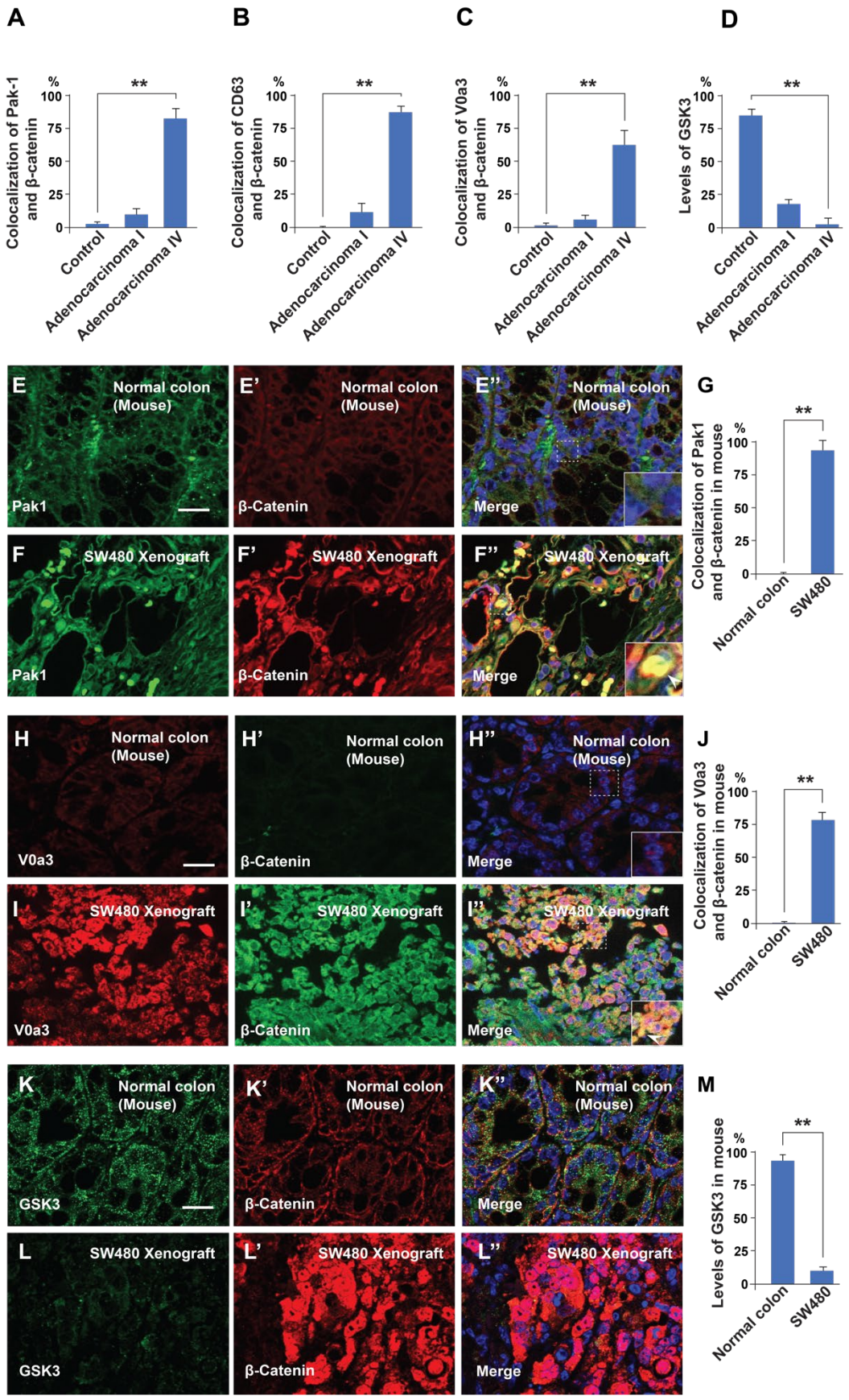
A
B
C
D
Colocalization of Pak-1 and β-catenin
Colocalization of CD63 and β-catenin
Colocalization of V0a3 and β-catenin
Levels of GSK3
%
100
75
50
25
0
**
Control
Adenocarcinoma I
Adenocarcinoma IV
E
E'
E''
Normal colon (Mouse)
Pak1
β-Catenin
Merge
F
F'
F''
SW480 Xenograft
G
Colocalization of Pak1 and β-catenin in mouse
Normal colon
SW480
H
H'
H''
V0a3
I
I'
I''
J
Colocalization of V0a3 and β-catenin in mouse
K
K'
K''
GSK3
L
L'
L''
M
Levels of GSK3 in mouse

Supplementary Figure S3. Malignancy of Colorectal Cancer Positively Correlates with Macropinocytosis, MVB, and Lysosome Markers, and Inversely Correlates with GSK3 Levels; Related to Figure 5

(A-D) Quantification of the colocalization between Pak1, CD63, V0a3, and GSK3 with β-catenin in normal colon and at different stages of cancer from the histological sections shown in Figure 5.
(E-E') Immunohistochemistry of normal colon tissue from the CD1 NU/NU nude mice stained for the macropinocytosis marker Pak1 and β-catenin.
(E'') Merge with DAPI.
(F-F'') SW480 xenograft showing correlation between high levels of Pak1 and β-catenin colocalization (see inset).
(G) Quantification of colocalization of Pak1 and β-catenin.
(H-H'') Control colon immunostained for V0a3 and β-catenin.
(I-I'') SW480 tumor showing a strong increase in the lysosomal marker V0a3 and β-catenin.
(K-K') Normal colon sample from mouse stained for GSK3 and β-catenin staining. Note that normal colon has GSK3 staining.
(L-L'') SW480 xenograft tumor showing reduced levels of GSK3, and high levels of β-catenin.
(M) Quantification of the levels of GSK3 in normal conditions and in tumor cells; note that the decrease in GSK3 levels supports the GSK3 sequestration model of Taelman et al. (2010).
Error bars denote SEM ($n \geq 3$) (**$P < 0.01$). (Scale bars, 10 μm). Human tissue arrays were quantfied in triplicate fields.

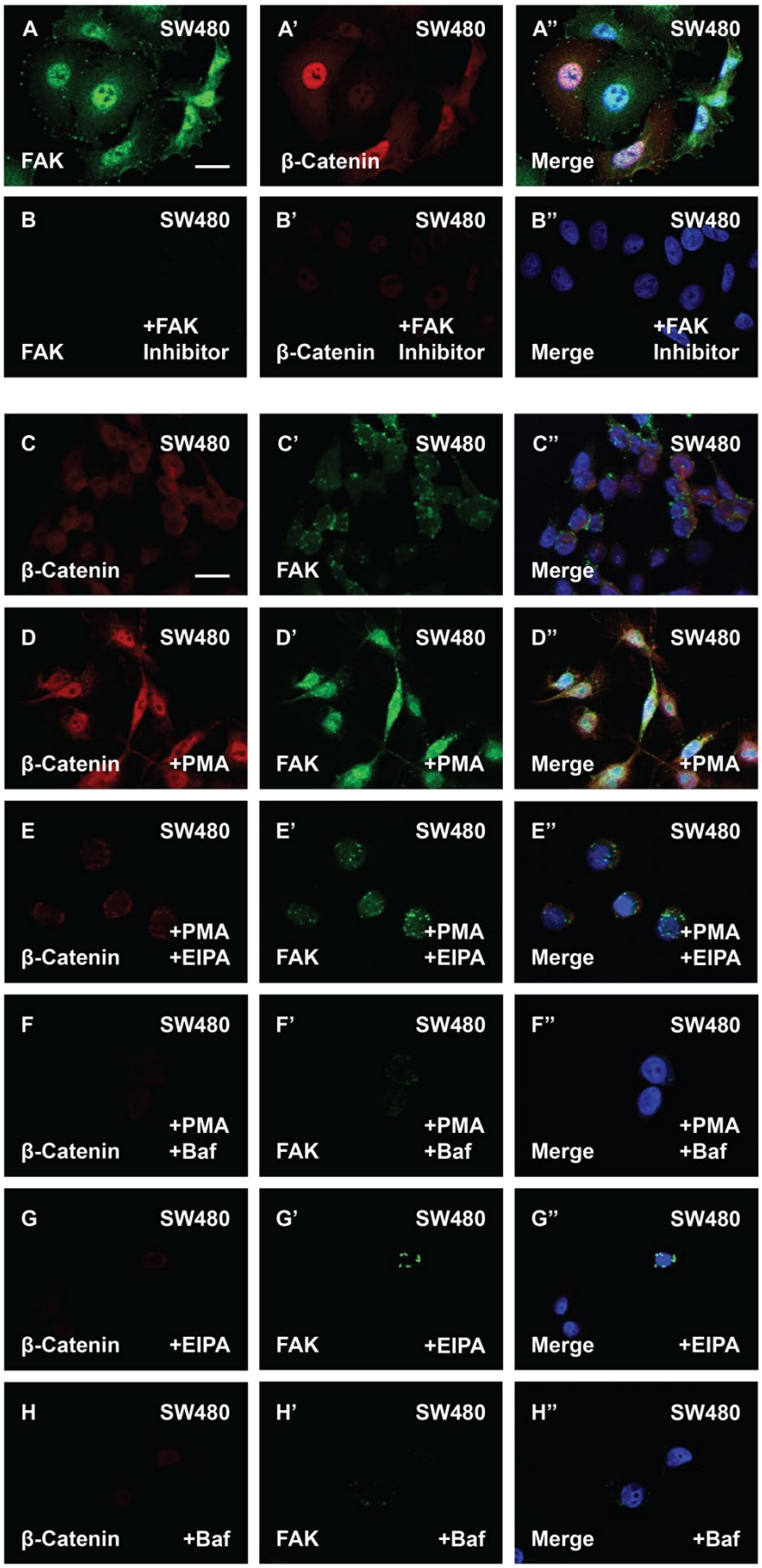
A SW480 FAK
A' SW480 β-Catenin
A" SW480 Merge
B SW480 FAK +FAK Inhibitor
B' SW480 β-Catenin +FAK Inhibitor
B" SW480 Merge +FAK Inhibitor
C SW480 β-Catenin
C' SW480 FAK
C" SW480 Merge
D SW480 β-Catenin +PMA
D' SW480 FAK +PMA
D" SW480 Merge +PMA
E SW480 β-Catenin +PMA +EIPA
E' SW480 FAK +PMA +EIPA
E" SW480 Merge +PMA +EIPA
F SW480 β-Catenin +PMA +Baf
F' SW480 FAK +PMA +Baf
F" SW480 Merge +PMA +Baf
G SW480 β-Catenin +EIPA
G' SW480 FAK +EIPA
G" SW480 Merge +EIPA
H SW480 β-Catenin +Baf
H' SW480 FAK +Baf
H" SW480 Merge +Baf

Supplementary Figure S4. The Phorbol Ester PMA Stabilizes FAK and enhances β-catenin levels in cells with constitutive Wnt signaling; Related to Figure 6

(A-A'') SW480 cells immunostained for FAK and total β-catenin antibody.
(B-B'') FAK inhibitor (100 nM) reduces FAK and β-catenin immunostaining levels.
(C-D'') SW480 cells treated with PMA showed increased in β-catenin and FAK levels. These images are the same as those in Figure 5K-L'', reproduced here as controls for the effects of membrane trafficking inhibitors in the same experiment.
(E-E'') EIPA (40 μM) overnight treatment blocked the effect of PMA in SW480 cells.
(F-F'') Baf (500 nM) treatment also blocked the effect of PMA in CRC cells.
(G-G'') EIPA treatment alone was sufficient to reduce β-catenin and FAK levels in SW480 cells.
(H-H'') Baf treatment in SW480 reduces β-catenin and FAK levels in SW480 cells.
Experiments in cultured cells represent biological triplicates. Error bars denote SEM ($n \geq 3$) (**$P < 0.01$). (Scale bars, 10 μm.).